Tu-Pos443

TWO DIMENSIONAL INFRARED CORRELATION SPECTROSCOPY OF THE MATURATION OF POORLY CRYSTALLINE HYDROXYAPATITE AT CONSTANT AND VARIABLE pH. ((Arne Gericke[1], Sergio J. Gadaleta[1], Joseph W. Brauner[1], Adele L. Boskey[2], and Richard Mendelsohn[1])) [1]Department of Chemistry, Rutgers University, Newark, N.J. 07102 and the [2]Hospital for Special Surgery, New York, N.Y. 10021

Recent publications from our laboratories report the FT-IR analysis of the ν_1, ν_3 phosphate region (900-1200 cm^{-1}) of poorly crystalline hydroxyapatite, the principle mineral phase in physiologically calcified tissue. The technique has been used to monitor the changes related to the maturation of poorly crystalline HA in both synthetic and biologic systems. One of the difficulties associated with analyzing spectra of poorly crystalline HA is that they are composed of several intrinsically overlapped bands which result in broad relatively featureless contours. To circumvent this problem a variety of techniques such as Fourier self-deconvolution, second derivative spectroscopy, and curve fitting have been used to elucidate the number and position of the underlying bands. However, each of the aforementioned techniques requires some degree of subjectivity in their respective applications. Recently, a generalized two-dimensional infrared (2D-IR) correlation method has been developed. This technique is capable of resolving the intrinsically overlapped bands in broad contours. The current work describes the use of 2D-IR for analysis of the ν_1, ν_3 phosphate region of maturing, poorly crystalline HA synthesized at constant and variable pH. Positions of the underlying bands elucidated by 2D-IR are compared with those from second derivative spectroscopy and Fourier self-deconvolution.

Tu-Pos444

CALCULATION OF VIBRATIONAL SPECTRA OF AMPHOTERIC SURFACTANTS. ((D. Grandbois, M. Trudel, and C. Chapados)) Département de chimie-biologie, Université du Québec à Trois-Rivières, Trois-Rivières, QC Canada G9A 5H7

Some amphoteric surfactants containing amino and carboxylic groups are of biological interests. While molecular spectroscopies are used more and more often to study the systems containing surfactants, the assignment of the bands used to probe the surfactant molecules is not completely done. To remedy the situation we have used a modified version of the computer program of Gribov and Dement'ev to calculate the ir and Raman spectra. The modified version that operates on an IBM RS6000 platform uses FORTRAN 90 as the programming language and is not limited by the number of atoms but only by the available memory of the computer. The molecular parameters of the molecule of interest which are obtained by Chem-X (Chemical Design, Inc.) are transported to the computer program where the position of the bands is calculated by the normal coordinate routines and the intensities by the electrooptical parameter routines. We have calculated the spectra of amines, carboxylic acids, and surfactants containing between 6 and 14 carbons. The comparison between experimental and calculated spectra is good. We will present the strategy used as well as the spectra obtained.

NUCLEIC ACID-PROTEIN COMPLEXES

Tu-Pos445

STRUCTURAL STUDIES OF A COMPLEX FORMED BY THE ROM PROTEIN AND A PAIR OF COMPLEMENTARY RNA STEM-LOOPS. ((A.J. Lee and D.M. Crothers)) Department of Chemistry, Yale University, New Haven, CT 06511. (Spon. by G. Brudvig)

Regulation of the replication for the Escherichia coli plasmid *ColE1* involves a plasmid encoded Rom protein and two RNA transcripts RNA I and RNA II, which function as antisense regulators of plasmid replication. Rom specifically recognizes an RNA loop-loop complex over standard A-form RNA and binds a bent helical RNA structure created by the interaction of the two stem-loops. Thus it negatively regulates the plasmid replication during the early stages of RNA I and RNA II interaction. Multidimensional heteronuclear magnetic resonance spectroscopy (NMR) was used for the initial analysis of the Rom-RNA complexes. The NMR data and the native gel electrophoretic analysis indicate that the RNA complex converts into duplex upon addition of the Rom protein.

Tu-Pos446

BINDING SITE IDENTIFICATION OF EUKARYOTIC PROTEIN SYNTHESIS INITIATION FACTOR EIF-4E USING A PHOTOAFFINITY ANALOG. ((D.E. Friedland[‡], C.H. Hagedorn[*], B.E. Haley[§] and D.J. Goss[‡])), [*]Dept. Of Medicine and Winship Cancer Center, Emory Univ. School of Medicine, Atlanta, GA 30322; [§]Dept. Of Medicinal Chem. And Pharmaceutics and the Markey Cancer Center, University of Kentucky Medical Center 40536; [‡]Chem. Dept., Hunter College , CUNY, NY, NY 10021.

Binding of eukaryotic initiation factors (eIF's) to the m^7(5')Gppp(5')N (where N indicates any nucleotide) cap structure at the 5' terminus of cellular mRNA represents the first committed step in the initiation phase of protein synthesis. Understanding the molecular basis for this recognition requires determination of the amino acids involved in the binding of the m^7G cap to eIF's. In order to investigate this, photoaffinity labeling with a cap analog [γ^{32}P]8N$_3$GTP was used in binding site studies of recombinant human cap binding protein ,eIF-4E. Competitive inhibition of this analog by m^7GTP and capped mRNA indicated probe specificity for interaction at the protein binding site. Aluminum (III)-chelate chromatography and reverse phase HPLC were used to isolate the photolabeled binding site peptide resulting from digestion of protein with modified trypsin. Subsequent amino acid sequencing results identified the amino acid sequence of the binding site peptide. In addition, sequencing results coupled with the inability to achieve trypsin digestion at a specific lysine indicate the individual residue which may be modified by [γ^{32}P]8N$_3$GTP.

Tu-Pos447

FLUORESCENCE AND CIRCULAR DICHROISM SPECTROSCOPIC CHARACTERIZATION OF WHEAT GERM PROTEIN SYNTHESIS INITIATION FACTOR EIF-4F AND ITS SUBUNIT P26 BINDING TO mRNA CAP ANALOGS. ((Y. Wang, T. Xiang, A. van Heerden[#], K.S. Browning[#], and D.J. Goss)) Dept. of Chem., Hunter College of CUNY, 695 Park Ave., NY, NY 10021; [#]Dept. of Chem., Univ. of Texas at Austin, Austin, TX 78712.

Recently the purified subunit p26, 26 kDa of wheat germ protein synthesis initiation factor eIF-4F has been obtained from *E. coli* expression of the cloned DNA. CD spectroscopy revealed 15% α-helix and 36% β sheet in p26 and 38% α-helix and 17% β sheet in eIF-4F. The binding of the 5'-terminal cap analog m^7GTP to p26 as a function of pH, temperature and ionic strength is described. The optimum binding pH was 8.0, ΔH and ΔS were 10.23 kcal/mol and 57.33 cal/mol°C, respectively. The environment of tryptophan residues in p26 and eIF-4F were monitored by using various quenchers. The results indicated the presence of negatively charged residues near the tryptophans which were surrounded by a hydrophobic environment in p26 and eIF-4F. The stopped-flow kinetics demonstrated the interaction of eIF-4F with m^7G cap followed a two-step mechanism. The rate constant and the activation energy for the second step were 121.7 s^{-1} and 4.55 kcal/mol, respectively.

Tu-Pos448

SPECTROSCOPIC STUDIES OF THE BINDING OF THE p28 AND P86 SUBUNITS OF WHEAT GERM INITIATION FACTOR, eIF-(iso)4F, TO eIF-4B AND TO mRNA. ((M.L. Balasta, M. Huang, Y. Wang, A. van Heerden[#], K.S. Browning[#] and D.J. Goss)) Chem. Dept., Hunter College (CUNY) New York, NY 10021; [#]Chem. Dept., Univ. of Texas at Austin, Austin, TX 78712.

Wheat germ protein synthesis initiation factor, eIF-(iso)4F, is a 110-kDa protein that is known to bind to mRNA and has exhibited ATP-dependent binding to oligoribonucleotides in the presence of eIF-4B and -4A. The p28 subunit of eIF-(iso)4F has been found to recognize and bind to the m^7G cap structure of mRNA, while the p86 subunit is believed to interact with other initiation factors and also with the mRNA. Direct fluorescence titration methods and circular dichroism spectroscopy was used to characterize the binding of the p28 and p86 subunits to eIF-4B, -4A and oligoribonucleotides. The oligoribonucleotide binding and CD spectra of several mutants of the p86 subunit were studied in order to further determine the role of the p86 subunit in protein-protein and protein-RNA interactions. Differences in alpha helical content have been observed among the mutants (by themselves or complexed with eIF-4B) and compared with p86. Equilibrium binding constants for the binary and ternary interactions involving p28, p86, eIF-4B and RNA indicate that initial binding of p86 or a p28:p86 complex with RNA enhances subsequent binding of eIF-4B to form the ternary complexes.

Tu-Pos449

Computational analysis of variants of the operator binding domain of the bacteriophage λ repressor.

((D.C. Kombo#, G. Ravishanker#, D.L. Beveridge#, and H.A. Scheraga*)). #*Department of Chemistry, Wesleyan University, Middletown, CT 06459.* * *Baker Laboratory of Chemistry, Cornell University, Ithaca, NY 14853-1301.*

In a continuing effort to understand the molecular basis of the dimerization-coupled DNA-binding activity of the bacteriophage λ repressor protein, we have analyzed conformational energy computations results on the wild type and its mutants with substitution in the dimer interface. We find that the hydogen bonds made by the peptide carbonyl oxygen of Tyr-85 to the peptide NH group of the residue at position 89 in active mutants are longer and less linear than their corresponding ones in inactive mutants. This behavior is due to the outward tilting of the carbonyl oxygen of Tyr-85 from the helix axis in active mutants, which in many cases result in disruption of its i to i+4 hydrogen bond involving this residue. The helical and hydrogen-bond parameters computed for both classes of mutants have been compared with the results obtained by others in the analysis of X-ray-derived crystal structures of α-helices in globular proteins. The results suggest that the carbonyl group of Tyr-85 in active mutants is presumably hydrogen bonded to a solvent molecule, whereas its counterpart in inactive mutants do not form such bonds. A rough correlation is also observed between the tolerance for amino acid substitution at position i of helix-5 with the number of close inter-monomer contacts involving the residues at position i and i-2. On the basis of these findings, we discuss the mutability of amino acid residues at the dimer interface.

Tu-Pos450

DNA SPECIFICITY AND THE STEROID HORMONE RECEPTORS.

((T. Bishop, D. Kosztin and K. Schulten)) Beckman Institute, UIUC, Urbana, IL 61801.

Molecular dynamics simulations have been conducted to investigate the binding of the steroid hormone receptor dimers to DNA. For this purpose simulations of complexes representing the glucocorticoid receptor DNA-binding domain (GR-DBD) and the estrogen receptor DNA-binding domain (ER-DBD) interacting with various target DNA segments have been conducted. The complexes are based on available X-ray structures of the GR-DBD/GRE4 and ER-DBD/ERE systems. A second set of simulations was conducted with the DNA segment altered for each system. For each simulation, the system was encapsulated in water. Protein-DNA interactions which distinguish an ER-DBD from a GR-DBD were evaluated during these simulations. DNA structural parameters were also analyzed for the GR-DBD/GRE systems and compared. "Ideal" biological systems are found to yield more favorable and symmetric protein-DNA interactions than the altered ones thus explaining the ability of the dimer to recognize its target DNA segment. Further analysis focused on deformations of the DNA that are induced in the target DNA segments GRE3 and GRE4 by the binding of the GR-DBD dimer. The deformations observed involve a 35° bend of the DNA, an unwinding and a displacement of the helical axis. These deformations are consistent with a mechanism for transcriptional regulation that involves a change of nucleosome packing upon GR binding. The protein-DNA interactions observed in our simulations include direct interactions between the target DNA segments and the three amino acids which distinguish an ER-DBD(E25, G26, A29 in human ER) from a GR-DBD(G458, S459, V462 in human GR).

Tu-Pos451

THERMODYNAMIC STUDIES OF *LAC* REPRESSOR-OPERATOR INTERACTION

((S. E. Melcher, D. E. Frank, M. M. Levandoski, O. V. Tsodikov, R. S. Spolar, and M. T. Record, Jr.)) Departments of Biochemistry, Chemistry, and program in Biophysics, University of Wisconsin, Madison, WI 53706

We are currently investigating several aspects of *lac* repressor's specific interaction with a symmetric operator. To probe how key interactions in the protein-DNA interface contribute to recognition, we have studied the affinity of several operator sequence variants for wild type repressor binding as a function of salt concentration and temperature. The contribution of DNA sequences outside the operator to the observed binding equilibrium is being investigated by changing the length of nonspecific DNA flanking the operator site. Finally, binding data as a function of solution conditions have been obtained for a wide range of repressor and operator concentrations to determine whether a dimer-tetramer equilibrium is linked to operator DNA binding. Contributions from sequence, length, and linked equilibria will be presented.

Tu-Pos452

THE DNA BINDING DOMAIN OF THE *ESCHERICHIA COLI* REPRESSOR OF BIOTIN BIOSYNTHESIS IS REQUIRED FOR TIGHT BINDING OF THE COREPRESSOR

((Yan Xu and Dorothy Beckett)) Department of Chemistry and Biochemistry, University of Maryland Baltimore County, Baltimore, MD 21228

The *Escherichia coli* repressor of biotin biosynthesis is an allosteric site specific DNA binding protein. The protein is composed of three structural domains. Contact with the biotin operator in the transcriptional repression complex is made by the N-terminal domain which contains a helix-turn-helix structural module. The central domain is required for the catalytic functions of BirA including synthesis of biotinyl-5'-AMP from substrates ATP and biotin and transfer of biotin from the adenylate to a lysine residue of the biotin carboxyl carrier protein of acetyl CoA carboxylase. The adenylate serves not only as the activated intermediate in the biotin transfer reaction but also as the positive allosteric effector for site-specific DNA binding. Little interaction between the N- and C-terminal domains is observed in the apo-repressor structure. In this work we have engineered an N-terminal deletion mutant of BirA , BirA65-321. Biochemical analysis of the purified truncated repressor indicates that, as expected, it does not bind to the biotin operator. BirA65-321 is, moreover, identical to intact BirA in catalysis of synthesis of bio-5'-AMP and in transfer of biotin from the adenylate to BCCP. Deletion of the DNA binding domain does severely compromise the ability of BirA to bind to biotin or bio-5'-AMP. The affinity of BirA65-321 for biotin is decreased 100-fold, while that for bio-5'-AMP is decreased 10000-fold relative to intact BirA. This significant functional role of the DNA binding domain in tight binding of the corepressor may be indicative of formation of extensive interdomain contacts in the holorepressor structure.

Tu-Pos453

THE *TRP* REPRESSOR OF *E. COLI*: PHYSICAL INVESTIGATIONS OF SUPER-REPRESSORS

((Ross J. Reedstrom†, Shyam Vangala*, Kathleen S. Martin‡, Erik W. Wilker* & Catherine A. Royer†*)) *University of Wisconsin School of Pharmacy and †Program in Cell and Molecular Biology Madison, Wisconsin 53706. ‡School of Pharmacy, Butler University, Indianapolis, Indiana.

Physical analysis of functional mutants of the *trp* repressor (TR) system have highlighted how the complex interplay of different equilibria all contribute to repressor function. Since few mutations affect a single characteristic in isolation, it is important to utilize a variety of physical techniques to investigate the each modification of TR. We have measured the physical state of mutant TR proteins by circular dichroism (CD), chemical denaturation, and 1,8-ANS binding, as well as probing the macromolecular interactions via fluorescence anisotropy and lifetime measurements of TR dilution and TR-DNA titrations. Here, we present investigations of five super-repressor mutants: EK13, EK18, DN46, EK49, and AV77 as well as wild-type TR. These studies demonstrate that super-repressor phenotypes may result from changes in operator affinity (DN46, EK49), protein-protein affinity (EK18), and the coupling of folding to ligand binding (AV77, EK13, EK18). Correlations between the oligomerization behavior and cooperativity of DNA binding for some of these mutants indicate that coupling of oligomerization to binding modulates the apparent cooperativity of binding to different operator sequences. This contributes to the independent control of affinity at sites of similar specificity necessary for coordinated, but differential, regulation of these operons.

Tu-Pos454

THERMODYNAMIC CHARACTERIZATION OF THE ASSOCIATION OF NF-IL6 bZIP TRYPTIC CORE DOMAIN WITH ITS SPECIFIC DNA SEQUENCE.

((A. R. Brasier, J. R. Casas-Finet and W. A. Wolfe)) Sealy Center for Molecular Science, UTMB, Galveston, TX 77555, and AIDS Vaccine Program, SAIC, NCI-FCRDC, Frederick, MD 21702. (Spon. by D. Kelman)

Nuclear factor IL-6 (NF-IL6) is a sequence-specific DNA-binding protein that contains a C-terminal basic domain-leucine zipper (bZIP) motif. Earlier proteolysis studies defined residues 266 and 345 as boundaries of a tryptic core domain (TCD) active in DNA binding. Equilibrium binding isotherms have been obtained monitoring the fluorescence polarization of a fluoresceinated DNA oligonucleotide carrying the angiotensinogen acute-phase response element (F-APRE M6) upon TCD binding. TCD bound to F-APRE M6 with a K_{obs} of 1.3×10^6 M^{-1} (16 mM NaCl, pH 7.5, 23 °C), and its affinity was markedly reduced by increasing [NaCl] (5×10^5 M^{-1} at 158 mM NaCl). The salt dependence of the binding affinity exhibited two distinct rectilinear phases in double-logarithmic plots, with an abrupt discontinuity *ca.* 65 mM NaCl. NaF, NaBr and $NaCH_3COO$ induced effects comparable to NaCl, with binding being the most stable in NaBr (K_{obs} = 2.0×10^8 M^{-1} in 16 mM NaBr). Complex formation in the presence of sodium glutamate appears qualitatively different than for other salts tested in that no discontinuity was observed between 16-158 mM. Biphasic salt dependence was observed with KCl, LiCl, and CsCl, at pH 6.0 or above, but became monophasic at pH 5.0. The extent of reduction in binding affinity was inversely correlated with cationic radii. ΔG decreased by 1.2 kcal/mol at pH 5.0, relative to pH 7.0, pointing to the involvement of titratable TCD side chains in the binding process. At pH 7.5 in 100 mM NaCl, point-mutated TCD D268A or D272A bound F-APRE M6 with greater affinity than TCD wt, suggesting that charged interactions occur between these acidic residues and DNA. Removal of res. 262-272 (the Complex Stabilizing SubDomain, CSSD) impairs DNA binding affinity. The fluorescence of a TCD mutant tryptophan-tagged upstream of the CSSD was quenched upon binding to wt APRE M6, by a non-radiative collisional deactivation of the indole excited state. Binding to $1,N^6$-ethenoadenylated APRE M6 sequences labelled at specific positions induced single-singlet energy transfer between Trp and εdA. The magnitude of this effect was maximal when the acceptor base was located within the *specific binding site* and decreased with either a proximal or distal location to this region, strongly suggesting that the donor Trp is in close proximity to the target DNA sequence.

Tu-Pos455

FLUORESCENCE, PHOSPHORESCENCE AND ODMR (OPTICALLY DETECTED MAGNETIC RESONANCE) INVESTIGATION OF THE NUCLEIC ACID BINDING OF NUCLEOCAPSID (NC) PROTEINS. ((J. R. Casas-Finet, M. A. Urbaneja, W.-C. Lam, A. H. Maki, and L. E. Henderson)) AIDS Vaccine Program, SAIC, NCI-FCRDC, Frederick, MD 21702, and Department of Chemistry, UCD, Davis, CA 95616. (Spon. by J. R. Casas-Finet)

Earlier luminescence studies of the Zn-finger NC proteins of HIV-1 (p7) and MuLV (p10) point to Trp stacking with nucleobases. Binding to single-stranded polynucleotides results in Trp fluorescence quenching, enhanced triplet state quantum yield, a red-shift of the phosphorescence 0,0-band, and a decrease of triplet lifetime and the D parameter in ODMR. Effects are positively correlated with increasing base affinity: G, I > T, U > C > A. Binding to poly(5HgU) results in a 1000-fold reduction in Trp triplet state lifetime, and the appearance of the D + E ODMR signal, induced by Hg. These effects are diagnostic of a van der Waals contact between Hg and the indole ring. Qualitatively similar effects are seen with $(5\text{-BrdU})_4$dT. We have extended this study to the SIV NC protein (p8), and investigated the effect of NCP metalation with divalent ions other than Zn(II). All NCPs bound DNA or RNA with an occluded site size of 6-7 bases. NCP affinity for a given oligonucleotide ranked: p8 ≥ p7 > p10. The higher affinity of double-finger NCPs (p7, p8) over single-finger ones (p10) stems from simultaneous interaction of both fingers with nucleic acids. ODMR results obtained with p8 show that its 2 Trp (1 per finger) undergo aromatic stacking upon nucleic acid binding. A conserved Tyr residue located in the Zn-finger motif of p10 shows extinction of its phosphorescence in the RNA complex, suggesting involvement of both Tyr and Trp in the binding process. Additional contributions of positively charged residues flanking the finger are inferred from the weak nucleic acid binding of a synthetic 18-aa p10 Zn-finger peptide. The Trp quantum yield of free NCPs ranked: Zn(II) > Cd(II) > apo > Co(II), suggesting dissimilar fluorophore microenvironment. $(dT)_4$ quenched the Trp fluorescence of p7 or p8 in their Zn(II) or Cd(II) forms by *ca.* 90%, but only ~ 40% for p10. For all NCPs, metalation with Cd(II) resulted in phosphorescence and ODMR results similar to the Zn(II) forms. Co(II), the ion with the largest radius in the series, imparts the lowest NCP binding affinity. Oxidized, disulfide-bonded p7 showed binding affinity and spectral effects intermediate between apo- and Zn(II)-p7. These results show the importance of a folded structure with a proper geometry for optimal activity.

Tu-Pos456

SPECTROSCOPIC STUDY OF THE SPECIFIC BINDING OF THE HIV-1 *gag* POLYPROTEIN AND NUCLEOCAPSID PROTEIN TO VIRAL RNAS ((S.C. Boydston-White,[1] S.P. Goff[2] and D.J. Goss[1]))

[1]Department of Chemistry, Hunter College of the City University of New York, New York, NY 10021
[2]Department of Biochemistry and Biophysics and the Howard Hughes Medical Institute, College of Physicians and Surgeons, Columbia University, New York, NY 10032

The HIV-1 *gag* polyprotein has been shown to be required for the dimerization of the HIV genomic RNA and the subsequent successful packaging of the virion. The interaction of the *gag* polyprotein with the Ψ region near the 5' end of the genome has been previously studied using riboprobes containing these sequences, via gel mobility shift assays. The nucleocapsid (NC) region of the *gag* polyprotein has also been shown to be necessary for the specific binding of the *gag* polyprotein, though the NC protein itself binds RNA in a less specific manner. Here, we have used fluorescence spectroscopy to determine the equilibrium constants of the binding of the complete *gag* polyprotein and that of the NC to riboprobes containing the HIV-1 Ψ sequences.

Tu-Pos457

Structure of an RNA-binding domain from ribosomal protein L11. ((Y. Xing and D. E. Draper)) Department of Chemistry, Johns Hopkins University, Baltimore, MD, 21218.

Ribosomal protein L11 and an antibiotic, thiostrepton, both recognize the same highly conserved, 58 nucleotide domain of 23S rRNA. A C-terminal, 75 amino acid fragment of *Bacillus stearothermophilus* L11 is found to have the same RNA binding properties as intact L11, such as stoichiometry, specificity, and dependence on Mg^{2+} and NH_4+ ions. However, the fragment lacks a cooperative interaction with thiostrepton which is seen with the intact protein. This suggests the existence of two functional domains in L11 protein. 2D and 3D NMR spectra of the C-terminal L11 fragment labeled with ^{15}N have been used to deduce the secondary and tertiary structure of this RNA binding domain.

Tu-Pos458

STRUCTURE STUDIES OF THE DNA-BINDING DOMAINS OF HAP1 AND THE MUTANT HAP1-18 BY NMR. ((M. Junker, K. H. Gardner, and J. E. Coleman)) Department of Molecular Biophysics and Biochemistry, Yale University, New Haven CT 06520-8114. (Spon. by R. M. Macnab)

The transcription factor HAP1 is involved in heme-induced expression of various genes in *Saccharomyces cerevisiae*. HAP1's DNA-binding domain contains a six cysteine sequence, C_{64}TICRKRKVKCDKLRPHCQQCTKT GVAHLC_{93}, conserved in 38 other fungal transcription factors and folding into zinc binuclear clusters in GAL4, LAC9, and PPR1. HAP1 differs from these latter transcription factors in having a longer spacing between the last two cysteines, with his-91 (a potential zinc ligand) inserted at the usual position of the last cysteine. In the HAP1 mutant HAP1-18, substitution of arginine for ser-63 alters DNA-binding specificity and increases transcription activation [K. S. Kim and L. Guarente (1989) *Nature 342:* 200]. We are using NMR to determine the structures of HAP1 and HAP1-18 fragments that contain the DNA-binding domain residues 62-99. Atomic adsorption indicates both fragments contain two zinc ions, as expected for binuclear clusters. Circular dichroism indicates the HAP1 fragment has structure similar to a comparable fragment of GAL4. In two-dimensional NOESY experiments with the HAP1 fragment, connectivities are evident among residues 62-99, indicating that the entire fragment is folded. Patterns of short-range NOESY connectivities reveal secondary structure elements found in other binuclear clusters, including short helices between residues 65-70 and 83-87 and a turn at pro-79. Determination of the tertiary folding of the HAP1 fragment, and of the structure of the HAP1-18 fragment, are being pursued. Detailed comparisons with structures of other binuclear cluster proteins will be made.

Tu-Pos459

UV RAMAN AND FLUORESCENCE SPECTROSCOPY STUDIES OF THE NUCLEOTIDE-BINDING DOMAIN OF THE IHF AND HU PROTEINS. ((I. Iliescu, M. Graettinger and I. Mukerji)) Department of Molecular Biology and Biochemistry, Wesleyan University, Middletown, CT 06459-0175

HU and Integration Host Factor (IHF) both belong to a histone-like prokaryotic family of proteins. These proteins, which have a high degree of sequence homology, have been implicated in the modulation of gene expression and repression. Both proteins putatively bind to the minor groove of DNA via two β-ribbon arms that extend from an α-helical core. An interesting feature of these proteins is that HU binds non-specifically to DNA, while IHF binds to a specific consensus sequence.

The factors conferring specificity to the IHF-DNA interaction have been investigated using a combination of fluorescence quenching and UV resonance Raman experiments. Preliminary results indicate that phosphate anions preferentially quench the fluorescence from aromatic residues relative to other anionic species. Removal of a non-conserved tyrosine residue (Tyr β93) located near the carboxy-terminus of the IHF β subunit was accomplished by proteolysis and measurements on the proteolyzed fragment indicate that this Tyr residue is spectroscopically distinct. Our results demonstrate that phosphate anions quench the fluorescence from the phenylalanine residues located in the dimeric core more than that from the Tyr β93 residue. These results are suggestive that the interaction with DNA is in part mediated through the deoxyribose-phosphate backbone and that Tyr β93 minimally participates in this backbone interaction. Specificity in binding is explicitly probed by comparing fluorescence and Raman results from IHF and HU.

Tu-Pos460

BINDING TO DNA OF CARBOXYL-TERMINAL PEPTIDES FROM HISTONE H1 VARIANTS. ((Susan E. Wellman)) University of Mississippi Medical Center, Jackson, MS 39216-4505

The carboxyl-terminal domains of the histone H1 proteins bind to DNA and are important in condensation of DNA. Little is known about the details of the interactions between H1 histones and DNA, and especially about differences among variant H1 histones in their interactions with DNA. Thermal denaturation of DNA was used to investigate differences in the binding affinities of peptide fragments from the carboxyl terminal domains of four non-allelic histone H1 variant proteins (mouse H1-1, H1-4 and H1°, and rat H1t). Three of the four peptides showed a slight preference for binding to a GC-rich region of a 214-base-pair DNA fragment, rather than to an AT-rich region. The fourth peptide, H1t, appeared to bind preferentially to the AT-rich region of the 214-base-pair fragment. The results show that these small peptides bind preferentially to a subset of DNA sequences; such sequence preference could extend to the intact H1 histones.

Tu-Pos461

LINKING ENERGETICS AND STRUCTURE OF DNA-PROTEIN BINDING THROUGH WATER RELEASE. ((N.Yu. Sidorova*&, E.G.Yarmola*& and D.C. Rau)) *Engelhardt Inst. Mol. Biol., Moscow, Russia, *LSB/DCRT and ODIR/NIDDK, NIH, Bethesda, MD 20892

Dissecting the molecular interactions underlying the formation of sequence - specific DNA-drug or DNA-protein recognition complexes requires linking thermodynamics and structure. We have been developing the Osmotic Stress technique as a tool for measuring the displacement of water, Δn_w, accompanying the association of DNA with proteins and drugs. Previously we showed that measuring competitive binding constants eliminated the initially seen dependence of Δn_w on the identity of the particular solute used to set water activity. Δn_w reflects a real difference in structure between the complexes. We have chosen three systems, restriction enzyme EcoRI, λ *cro* protein and the antibiotic netropsin, for measuring systematically the dependence of binding energy to DNA to different sequences on Δn_w. We measure the ability of EcoRI star-sites to compete with the EcoRI cleavage site for nuclease binding and the ability of *cro* mutant operators to compete with the consensus sequence for *cro* protein binding. Competitive binding constants are measured using the gel mobility shift assay. The ability of different sequences to compete with the EcoRI cleavage site for the netropsin binding is monitored using a restriction enzyme protection assay. In each case the tighter the complex the more waters are released.

Tu-Pos462

Application of Atomic Force Microscopy to study DNA-Protein interactions((S. Nettikadan@,#, H. Yu#, F. Tokumasu#,*, P. Kolattukudy@,#, K. Takeyasu@,#)) #Neurobiotechnology center, *Department of Biophysics and @Department of Medical Biochemistry, The Ohio State University, Columbus, OH. 43210

DNA-Protein interaction plays a vital role in the transcriptional regulation of gene expression. The conformational changes induced by the protein on binding to DNA are proposed to play an important role in its function. The functional aspects of many transcription factors have been characterized. Here we report the successful application of Atomic Force Microscopy (AFM) to study the direct binding of a recombinant palindromic binding protein to a specific site on fungal cutinase promoter (Figure) and the molecular interaction between transcription factors (Sp1 and Ap2) and 5' regulatory region (up to 3.4 kb) of the Na, K-ATPase alpha-subunit gene.Our results demonstrate the possible applications of AFM to such DNA-Protein Interactions in; i) Mapping of the recognition sites of specific DNA binding proteins over several kb of target DNA, ii) Detection of multimerization of DNA binding proteins, iii) Detection of interaction between different DNA binding proteins and iv) Detection of the conformational changes induced by DNA binding protein upon binding to DNA.

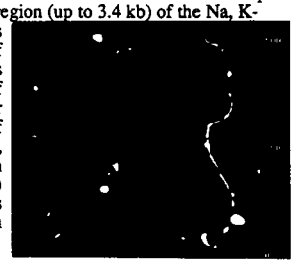

Tu-Pos463

ROLE OF AMINO ACID RESIDUES IN THE RECOGNITION HELIX OF THE NK-2 HOMEODOMAIN ON STRUCTURE, FUNCTION AND THERMAL STABILITY ((S. Weiler, D. Tsao, J. Gruschus, L. Yu, L.-H. Wang, M. Nirenberg and J. Ferretti.)) NHLBI, NIH, Bethesda, MD 20892.

The NK-2 homeodomain protein is a 60 amino acid residue part of a 723 residue protein that is expressed early in Drosophila embryonic development in part of the central nervous system. The NK-2 homeodomain binds to the unusual consensus sequence, TCAAGTG. This binding results in an elongation of the recognition helix as determined by our solution structures in the free and DNA-bound states. To understand the role of individual residues, amino acids at non-conserved positions in the recognition helix were substituted for their respective counterparts in the Antennapedia homeodomain. A Y54M mutant protein displayed a drop in binding affinity by an order of magnitude compared to the wild type homeodomain. No decrease in binding affinity was observed for H52R and T56W single mutants, nor for the corresponding double mutant. Circular dichroism experiments revealed no significant structural difference between the wild type and Y54M mutant proteins. However there was a marked increase in the molar ellipticity at 222nm for the double mutant. Furthermore the melting temperature observed for the double mutant was 33^0C compared to 25^0C for the wild type protein. The role of these residues in the elongation of helix III is examined by high resolution NMR experiments.

Tu-Pos464

EFFECTS OF MPD ON DNA CURVATURE. ((M. Dlakic and R.E. Harrington)) Department of Biochemistry, School of Medicine, University of Nevada Reno, Reno, NV 89557-0014 USA

The origin of DNA curvature, although studied extensively, remains unclear. It was originally thought that DNA curvature arises from additive bending contributions of periodically spaced A-tracts (Crothers *et al.*, 1990). However, it has been proposed (Goodsell *et al.*, 1994), based on crystallographic results, that A-tracts are straight, while other sequence elements are bent (bent non-A-tract model). Sprous et al. recently showed that 2-methyl-2,4-pentanediol (MPD), the dehydrating reagent commonly used in crystallography, reduces the curvature in A-tracts (Sprous *et al.*, 1995). Using 2D cyclization assays, gel mobility experiments, and chemical probing on sequences with and without A-tracts, we tested whether MPD might be the reason for differences observed in crystallographic studies vs. solution and gel mobility experiments. We show that MPD effects are specifically directed to A-tracts. Our results strongly suggest that crystallographic results on the sequences with A-tracts must be interpreted with caution when MPD is used in crystallizing. It seems that its main effect might be straightening of A-tracts, which leads to the reversal of gel mobility anomaly, reduced efficiency of cyclization, and changes in cutting profiles within A-tracts observed here.

Crothers *et al.* (1990) *J. Biol. Chem.* **265**, 7093-7096.
Goodsell *et al.* (1994) *J. Mol. Biol.* **239**, 79-96.
Sprous *et al.* (1995) *Nucleic Acids Res.* **23**, 1816-1821.

Tu-Pos465

DNA DISTORTION BY THE METALLOREGULATORY PROTEIN MerR EXAMINED USING CYCLIZATION KINETICS ((Michael D. Reigle' and Thomas V. O'Halloran*)) 'Department of Biochemistry, Molecular Biology, and Cell Biology and 'Department of Chemistry, Northwestern University, Evanston, IL 60208.

Bacterial mercury resistance genes are regulated by the protein MerR, a transcriptional repressor that switches to an activator in response to submicromolar amounts of mercuric ion. The switch is thought to be the result of a mercuric ion-induced change in protein conformation, which is translated into distortion of the operator. Helical phasing experiments showed a protein-induced bend that is lost upon addition of mercuric ion, which contradicted circular permutation studies that showed a bent operator in the presence and absence of mercuric ion. Cyclization kinetics have the advantage of being solution based studies, and have been used extensively to study the physical properties of DNA. We have studied the effects of MerR binding on the cyclization kinetics of DNA, both in the presence and absence of mercuric ion.

Tu-Pos466

FLUORESCENT PTERIDINE NUCLEOSIDE ANALOGS AS PROBES FOR MONITORING PROTEIN/DNA INTERACTIONS: ((M.E. Hawkins[1], W. Pfleiderer[2], J.R. Knutson[3], D. Porter[3], and F. Balis[1])) [1]NCI, NIH, Bethesda, MD, [2]Universität Konstanz, Fakultät für Chemie, Konstanz, Germany, [3]NHLBI, LCB, NIH, Bethesda, MD 20892.

We have developed a series of pteridine-based, fluorescent nucleoside analogs that are suitable for automated, site-specific incorporation into oligonucleotides. Quantum yields (relative to quinine sulfate) of 18 pteridine deoxyribo- or ribo-nucleoside analogs measured in aqueous buffers, pH 6- 8, ranged from ≤ 0.03 to 0.88. 3-Methyl-isoxanthopterin (3-MI) and 6-methyl-isoxanthopterin (6-MI) were synthesized as 2'-deoxy-5'-O-dimethoxytrityl-β-D-ribofuranosyl phosphoramidites and incorporated into single strand oligonucleotides. Incorporation caused significant quench (>84%), and the degree of quench correlates both with the number and proximity of neighboring purines and the position of the fluorophore in the strand. Incorporation of 3-MI perturbs annealing, as evidenced by a melting temperature (Tm) depression equivalent to that of a single base pair mismatch at the identical positions. Although the fluorescence of 6-MI was quenched similarly to 3-MI, the Tm's of 6-MI-containing double strands were identical to unlabeled oligonucleotides, suggesting that 6-MI is capable of base pairing. 6-MI also exhibited a distinct shift in absorbance, emission and decay associated spectra at different pH values. This class of mid-UV to blue quasi-intrinsic probes should help provide new insights into protein/DNA interactions.

Tu-Pos467

MODELING ELECTRON TRANSFER IN REDOX PROTEINS: A BINARY TUNNELING BARRIER MODEL. ((C.C. Page, R. S. Farid, C. C. Moser and P. L. Dutton)) University of Pennsylvania, Johnson Research Foundation, Dept. of Biochem./Biophysics, Philadelphia, PA, 19104.

We have developed a method that examines the protein atomic structure between cofactors in electron transfer proteins, and calculated optimal electron transfer rates for the photosynthetic reaction centers of *Rhodopseudomonas viridis*. Comparison with previously measured rates (Moser *et al. Nature*, **335**, 796-802 (1992).) show reasonable agreement for most of the reactions, with two instructive deviations. Electron transfer between Q_a and Q_b was found to be some 10^3 fold faster than measured, while that between bacteriopheophytin (BPh) and the bacteriochlorophyll dimer ($BChl_2$) was found to be 10^3 slower than measured. The method was extended to calculating electron transfer rates between other cofactors for which rates have not been measured. These include rates between the four hemes, down the L-branch, and between the L- and M-branch BPh and BChls. These rates also do not deviate far from expectations based on an average β value of 1.4 Å.

Tu-Pos468

DESIGN AND SYNTHESIS OF A [4FE4S] PROTEIN ((S. E. Mulholland, B. R. Gibney, F. Rabanal, P. L. Dutton)) Johnson Research Foundation, Department of Biochemistry and Biophysics, University of Pennsylvania, Philadelphia, PA 19104

We have successfully designed, synthesized and partially characterized an α-helical peptide which binds a [4Fe4S] cluster. This peptide is a *de novo* designed four helix bundle that contains a total of six redox cofactor binding sites, four for bis-histidine ligated hemes within the helical framework and two for [4Fe4S] type clusters within loop regions. The peptide was synthesized as a 67 amino acid helix-turn-helix peptide that aggregates as a four helix bundle in solution. The iron-sulfur binding site was added by placing a seven amino acid loop containing three of the four cysteine ligands between a pair of helices. The sequence of this loop was based on native ferredoxins with a sequence of CIACGAC. The fourth cysteine ligand is derived from a remote site located at the top of one of the alpha helices. The bound iron-sulfur cluster is EPR silent as isolated, but upon reduction has a rhombic EPR spectrum similar to those of natural [4Fe4S] clusters with g values of 2.06, 1.93 and 1.89. The power saturation and temperature dependencies of this cluster are also comparable to those observed for natural ferredoxins. The cluster has a measured E_{m8} of less than -400mV consistent with native ferredoxins. This peptide successfully bound both hemes and the iron-sulfur clusters with all six sites filled. This work demonstrates how a four helix bundle can be used as a stable scaffold to which a short natural peptide sequence can be attached with retention of metal binding capabilities.

Tu-Pos469

RESONANCE RAMAN STUDIES OF INHIBITORS AND INHIBITOR SOLVENTS EFFECT ON RHODOBACTER CAPSULATUS bc_1 COMPLEXES. ((F.Gao[a], H. Qin[b], D.B.Knaff[b], M.C. Simpson[c], J.A. Shelnutt[c] and M.R. Ondrias[a])) a: Dept. of Chem., Univ. of N.M., Albuquerque, NM 87131. b: Dept. of Chem. and Biochem., Texas Tech Univ., Lubbock,TX 79409. c: Sandia National Lab, Albuquerque, NM 87185

The effects of electron transfer inhibitors on the local environment of the cytochrome active sites in bc1 complexes were examined by Resonance Raman(RR) and Raman Difference Spectroscopy (RDS). Selective excitation and partial reduction were used to isolate and quantify changes in the vibrational spectra of hemes b_H, b_L and c_1. Our results demonstrate that the binding of inhibitors to either Q_O or Q_P sites does not dramatically alter the equilibrium structure of hemes b_H and b_L, but does affect both the photodynamics and stability of the complex in mixed solvent systems.
(Supported by the NIH (GM 33330 to MRO), USDA (to DBK), DOE Dist. Postdoc Fellowship (to MCS), and DOE (DE-AC04-94AL 85000 to JAS))

Tu-Pos470

Characterization and Electron Transfer studies on a Coordination Complex Between Microperoxidase-11 and Ruthenium trisbipyridine derivatised Bifunctional Peptides (B. Fan[a], R. W. Larsen[b], C. Simpson[c], S. Niu[b], R. Falcon[a], L. Marteniz[a], D. L Fontenot[d], M. Ondrias[a]) a Chemistry Department, University of New Mexico; b Chemistry Department, University of Hawaii at Manoa; c Fuel Sciences Division, Sandia National Laboratories, and d Life Sciences Division, Los Alamos National Laboratories.

A novel series of ruthenium trisbipyridine derivatized peptides are used to assemble a electron transfer model complexes with microperoxidase-11, in which the ruthenium group serves as the photoelectron donor separated from the heme acceptor by varying numbers of proline residues(n=1 to 3). Transient resonance Raman spectra of the complexes sample show clear evidence of photoinduced electron transfer (ET) within 10ns laser excitation. More interestingly, the ET process are accompanied by complicated structural dynamics like ligand photolysis under high laser flux. Time resolved luminescence was employed to estimate both the ET rate constants and the binding constants. The ET rates such derived are 4.6×10^7, 2.2×10^7 and 4.3×10^6 s^{-1} for the three peptides studied. The center-center separation dependence of the system gives a α value of 0.9 A^{-1}, which falls within the lower end of the values observed in the other systems. (Supported by the NIH GM3330 to MRO)

Tu-Pos471

SITE-DIRECTED MUTAGENESIS OF THE UBIQUINONE-BINDING AMPHIPATHIC HELIX IN THE CYTOCHROME *b* PROTEIN OF THE CYTOCHROME *b*-c_1 COMPLEX FROM *RHODOBACTER SPHAEROIDES* ((M. W. Mather, C.-A. Yu and L. Yu)) Dept. Biochem. & Molec. Biol., Oklahoma State University, Stillwater, OK 74078-3035

Residues 158-171 of *R. sphaeroides* cytochrome *b* (*b*) correspond to a ubiquinone-binding peptide identified by photoaffininty labeling studies on the mitochondrial cytochrome *b*-c_1 complex (bc_1). These residues are thought to form part of an amphipathic helix, which participates in the formation of the quinol oxidizing (Q_o) center. We have prepared a series of largely conservative substitutions in the 157-171 span of *b*. None of these amino acids is absolutely required for growth or enzymatic activity. However, substitutions at several positions have a significant effect on the properties of the bc_1. The sensitive residues do not cluster on one side of the amphipathic helix. Substitutions at positions W157, G158, T160, L165, F166, and P170 generally lower the enzymatic activity, but some changes at I162 increase the maximal activity. We have purified several of the altered bc_1's. The apparent kinetic parameters of the purified complexes are similar to the values measured in the native membranes; in several cases the apparent Km's of the substituted bc_1's for ubiquinol are lower than that of the native complex, suggesting tighter binding of ubiquinol. EPR spectra of several altered complexes indicate an altered interaction between the Q_o center and the iron-sulfur cluster in the Rieske protein. In the case of T160→S, EPR also suggests a long-range interaction with b_{562}. Changes in this region (especially at T160) may also affect the interaction between *b* and subunit IV of the complex. Since alterations throughout the region appear to affect the properties of the active centers and subunit interactions, the 157-171 span of *b* must have a pivotal role in the structure and function of the cytochrome bc_1 complex. Supported in part by NIH grant GM 30721 (CAY) and OCAST grant HN3-008 (MWM).

Tu-Pos472

INTERMEDIATES IN THE REACTION OF CYTOCHROME c OXIDASE WITH DIOXYGEN: A FLOW-FLASH STUDY USING MULTICHANNEL TRANSIENT ABSORPTION SPECTROSCOPY. ((Artur Sucheta and Ólöf Einarsdóttir)) Department of Chemistry and Biochemistry, University of California, Santa Cruz, CA 95064.

The reaction of fully reduced cytochrome oxidase (CcO) with dioxygen was studied by flow-flash transient optical absorption spectroscopy. The reaction was initiated by laser flash photolysis of CO from the fully reduced CcO in the presence of 625 mM O_2. A gated optical multichannel analyzer was used to collect transient difference spectra in the Soret and alpha regions at delay times between 50 ns and 500 ms after CO photolysis. The resulting arrays of ΔA as a function of wavelength, λ, and delay, Δt, were treated by singular value decomposition (SVD) which provided insight into the order of appearance and the minimum number of components in the reaction mixture. Multiexponential fitting yields the following apparent lifetimes: (1.0±0.2) µs, (15±5) µs, (30±5) µs, (80±10) µs and (1.2±0.1) ms. The 1 µs process is attributed to a conformational change at cytochrome a_3. The processes at ~15-30 µs likely reflect the binding of oxygen to cytochrome a_3, followed by oxidation of cytochrome *a*. On the 100 µs time scale, a species with an absorption maximum at 580 nm ("ferryl form") reaches maximum concentration. At 1.2 ms, the prevalent process is oxidation of cytochrome a_3. We propose a sequential model to account for the experimental behavior and present microscopic rate constants and spectra of the reaction intermediates. Supported by NIH grant R29 GM45888.

Tu-Pos473

THERMOKINETIC SIMULATION OF THE Q-CYCLE. ((C. Wagner, D.Walz)) Biozentrum Univ. Basel, CH-4056 Basel, Switzerland.

The bf-complex is situated in the thylakoid membrane and functions as plastoquinol-plastocyanin oxidoreductase in the photosynthesis of chloroplasts. It contains two electron pathways. The high potential chain leads along the intrathylakoid surface of the membrane and links photosystem II with photosystem I. The low potential chain is composed of two hemes located in the b cytochrome which mediates the electrons across the membrane from the plastoquinol oxidizing site, Q_o-site, at the lumenal side of the membrane to plastoquinone reducing site, Q_i-site, at the stromal side. The plastoquinol /quinone system together with the low potential chain constitute the Q-cycle.
We simulated the Q-cycle by a 48 state model. The reaction rate constants for intramolecular electron transfer reactions are calculated by means of the Marcus theory and the rate constants for the dissociations are taken from literature. The model incorporates instable plastosemiquinones at the Q_i- as well as at the Q_o-site.
Recently we have presented a model which allows one to deconvolute the absorbance change of potentiometric titration experiments in terms of interacting redox centers. It was included in the simulations, compared to non-interacting redox centers and its implications on the dynamics of the system are explored.

Tu-Pos474

EXPRESSION OF THE COFACTOR BINDING SUBUNITS OF THE PROTON-TRANSLOCATING NADH-QUINONE OXIDOREDUCTASE (NDH-1) OF *PARACOCCUS DENITRIFICANS*. ((1Yano, T., 2Sled', V.D., 3Johnson, M.K., 2Ohnishi, T., and 1Yagi, T.)) 1TSRI, La Jolla, CA 92037, 2Univ. of Pennsylvania, Philadelphia, PA 19104-6089, 3Univ. of Georgia, Athens, GA 30602-2556.

A Gram negative soil bacterium, *Paracoccus denitrificans*, possesses the proton-translocating NADH-quinone oxidoreductase (NDH-1) whose enzymatic and molecular properties are very similar to those of mitochondrial Complex I. The *P. denitrificans* NDH-1 is composed of at least 14 dissimilar subunits (NQO1-14) and contains one molecule of FMN and at least 5 EPR-visible FeS clusters (N1a, N1b, N2, N3, and N4) as prosthetic groups. In order to deepen our understanding of the reaction mechanism of the enzyme complex, it is a prerequisite to identify the number and location of the cofactors and to characterize them at a molecular level. We hypothesize that NQO1, 2, 3, 6, and 9 are cofactor binding subunits. In order to verify the supposition, we have attempted to express these putative cofactor binding subunits individually in *E. coli* and have characterized the coordinated cofactors with several physicochemical measurements. The results obtained so far were summarized in Table.

These results seem to make the NQO9 subunit a more plausible candidate for the location of center N2. The subunit contains two repeated consensus sequence motifs for the [4Fe-4S] cluster binding site. Therefore, we attempted to express the NQO9 subunit in *E. coli*. The subunit was overexpressed as insoluble products. Preliminary results of EPR analysis, however, revealed that the expressed subunit contains two species of iron-sulfur clusters: a [4Fe-4S] cluster with axial symmetry (E_m=-200mV) and a [3Fe-4S] cluster (E_m=+70mV). We also found that when Fe ions were reconstituted *in vitro*, the subunit exhibited EPR spectra very similar to those of 8Fe ferredoxins. Further characterization of the expressed subunit is in progress in our laboratories.

Table Localization of cofactors

	Pd NDH-1	Mt Complex I	Cofactor
FP	NQO1	51kDa	NADH-binding site, FMN-binding site (?), [4Fe-4S] (N3)
	NQO2	24kDa	[2Fe-2S] (N1a)
IP	NQO3	75kDa	[2Fe-2S] (N1b), [4Fe-4S] (N4), [4Fe-4S] (S=3/2)
	NQO6	20kDa (PSST)	FeS cluster (?)
HP	NQO9	23kDa (TYKY)	2x[4Fe-4S] (N2?)

Tu-Pos475

THE THREE DIMENSIONAL STRUCTURE OF MOUSE RECOMBINANT NAD(P)H: QUINONE REDUCTASE
M. Faig*, M. Bianchet*, S. Cheng**, and L. M. Amzel**Dept. of Biophysics and Biophysical Chemestry. Johns Hopkins University.**Division of Immunology Beckman Research Institute of the City of Hope

The Quinone Reductase (EC.1.6.99.2) also called DT diaphorase, is a flavoprotein that catalyzes the two electron reduction of quinones and quinoids using NADH or NADHP as electron donors. Evidence shows that this protein could be an important chemo-protector agent against the carcinogenic effect of quinones. The 3-D structure of mouse protein in the presence of FAD was solved by X-ray diffraction methods. It has been reported that QR activity depends on the species. However the activities of human and mouse enzymes are very similar, at least with respect to their ability to convert products of the nitrobenzene prodrug CB 1954 into a single product such as 5-(azi-ridin-1-yl)-4-hydroxylamino-2-nitrobenzamide. In contrast with the rat the reduction rate of the same compound is five and half times greater. The differences between rat, mouse and human are discussed.

CELL MOTILITY

Tu-Pos476

MODELLING THE SPECIAL FEATURES OF THE MAMMALIAN SPERM AXONEME. ((C. B. Lindemann)) Department of Biological Sciences, Oakland University, Rochester, MI 48309.

The flagellum of a mammalian sperm has features that distinguish it from simple flagella. The axoneme has extra elements called outer dense fibers (ODFs) that are attached to the outer doublets. These ODFs are anchored into a connecting piece at the flagellar base; while the outer doublets are not attached to a basal centriole, as they are in simple flagella. Given this geometry, the forces generated by dynein-tubulin sliding are likely to be transferred to the ODFs, which in turn transmit these bending forces to the connecting piece. Sliding of the doublets under these circumstances is governed by the ODF spacing. The greater spatial separation of the ODFs (compared to the outer doublets) increases both the magnitude of the bending torque and the amount of interdoublet sliding occurring during a flagellar beat. The inter-ODF spacing of bull sperm was used to modify a flagellar model based on a simple axoneme (Lindemann, 1994, *Cell Motil. Cytoskeleton*, **29**:141-154). When the model was scaled to the length and stiffness of a bull sperm, the resultant simulation closely resembled the beating pattern of live bull sperm. The model demonstrates that the ODFs act to consolidate the energy from more dynein cross-bridges into the production of a single bend. Compared to a simple 10 μm cilium, bending is powered by 8 × more dyneins acting together to produce an 18 × larger bending moment. Thus, the same central 9 + 2 axoneme can power a much larger (and stiffer) flagellum than would otherwise be possible. Supported by N.S.F. Grant MCB-9220910.

Tu-Pos477

ROLE OF CROSSLINKER GEOMETRY IN THE FORMATION OF ISOTROPIC VERSUS BUNDLED ACTIN FILAMENT CLUSTERS. ((P.A. Dufort and C.J. Lumsden)) Department of Medicine, University of Toronto, Toronto, Canada, M5S 1A8. (Spon. by C.J. Lumsden)

The actin cytoskeleton and its associated regulatory proteins are the key mediators of changes in cell structure and viscoelasticity. Despite the apparently unlimited number of three-dimensional structures into which actin filaments could conceivably be organized, actin filaments *in vivo* are most often found in one of only two distinct arrangements: tight bundles of many parallel filaments, or loose networks in which different filaments possess all possible orientations. We describe the results of a Brownian dynamics simulation study designed to explore the role of crosslinker geometry in the creation and maintenance of actin filament clusters possessing either or both of the parallel and isotropic filament arrangements. The model simulates the translational and rotational diffusion of actin filaments, and the formation of crosslinks that bind pairs of filaments either in parallel or at right angles. We have run 6 sets of 10 simulations as follows: 3 sets with short (112 nm) filaments and 3 sets with longer (225 nm) filaments, and within these 2 groups of 3, one set with parallel crosslinkers, one set with right-angle crosslinkers, and one set with both types of crosslinker. Our results suggest that the principal determinant of actin filament cluster morphology is filament length. When parallel and right-angle crosslinkers must compete for a limited number of F-actin binding sites, right-angle crosslinkers will dominate when filaments are short, resulting in isotropic networks, while parallel crosslinkers will dominate when filaments are long, resulting in parallel bundles.

Tu-Pos478

VARIATION OF THE RATE OF EXTENSION OF ACTIN NETWORKS IN THE BROWNIAN RATCHET MODEL.
((D. J. Olbris and J. Herzfeld)) Brandeis University, 415 South St., Waltham MA 02254-9110.

The acrosomal process of the sea cucumber *Thyone* may extend 90μm in 10 seconds, and epithelial goldfish keratocytes may glide less than 0.01 μm in 1 second. Yet the speed of both is believed to derive from the rate of extension of an actin network. We examine an existing model, the Brownian ratchet [Peskin *et al.*, Biophys. J. **65**, 316 (1993)], with an eye toward explaining this wide range of extension speeds. In the model, actin polymerization renders the Brownian fluctuations of a membrane unidirectional, resulting in forward extension. Not addressed by the model are (1) the delivery of actin monomers to the extension front, and (2) the effects of the concentration gradients that arise when spatially localized polymerization occurs. These aspects are coupled: concentration gradients cause diffusive and convective flows that affect the delivery of actin monomers. Through this causal chain, variation of the actin polymerization rate constant can control the delivery of monomers to the forward region and thus sustain varying speeds. of the Brownian ratchet. This mechanism can predict the wide range of observed extension speeds.

Tu-Pos479

A TABLE-TOP FLASH CONTACT X-RAY MICROSCOPE SYSTEM
((H. Shimizu, T. Majima, T. Tomie, A. D. Stead*, T. Ford*, K. Miura, M. Yamada and T. Kanayama)) Electrotechnical Laboratory, Tsukuba, JAPAN and London University*, U. K. (Spon. by H. Matsumura)

A table-top flash contact x-ray microscope system was constructed. The system consists of a table-scaled YAG laser for producing a plasma which emits x-rays and a small vacuum chamber with sample holder. This has enabled us to obtain x-ray microscopy images of living specimens in our own laboratory without the need for SR sources or large laser facilities. The performance of the system is demonstrated by presenting x-ray images of unicellular alga Chlamydomonas, Tetraselmis and Phytomonas in water. The subcellular structures, such as basal part of flagella, are visible in the x-ray image. The Chlamydomonas images also show dividing mother cells with daughter cells. These results demonstrate that the x-ray microscopy can be powerful for the observation of living materials and that large facilities are unnecessary.

Tu-Pos480

EVIDENCE THAT ACTIN NUCLEATING FACTOR (ANF) CONTAINS ACTIN
((L.C. Gershman[§¶‡], L.A. Selden[§], H.J. Kinosian[¶], and J.E. Estes[§¶],))
[§]Research and [‡]Medical Services, Department of Veterans Affairs Medical Center, Albany, NY 12208 and Departments of [‡]Medicine and [¶]Physiology and Cell Biology, Albany Medical College, Albany, NY 12208.

We previously reported that ANF, a contaminant in rabbit skeletal muscle preparations, acts by stabilizing actin nuclei (Biophys. J. 66: A196 (1993)). Certain observations suggest that ANF may contain actin. The time course for loss of ANF activity is ATP dependent and parallels the time course of actin monomer denaturation. Sepharose-bound DNase I added to actin solutions containing ANF removes ANF activity in direct proportion to the amount of actin removed. The activity associated with ANF correlates with a 140 kDa protein band on reduced PAGE analysis, but we have been unable to purify the active 140 kDa band free of monomeric actin. Since monomeric actin is always the major protein in ANF preparations, we investigated whether ANF activity was caused by the 140 kDa protein rather than by an altered form of monomeric actin. We centrifuged ANF fractions stabilized with 5 mg/ml dextran (MW 80 kDa) in an airfuge rotor for 6 hours and assayed the top 25 % of the tube for actin and ANF activity. The actin concentration in the top layer was reduced by 25%, while the ANF activity was reduced by 95%. Most of the ANF activity could be found in the bottom 25 % of the tube, suggesting that ANF activity is caused by the 140 kDa band. To address the similarities between ANF and actin we used antibodies directed to the N-terminus and C-terminus of actin to probe western blots of active fractions. We found that the 140 kDa band reacts with both antibodies. Thus far we have not observed any non-actin component of ANF in ANF samples, leading to the possibility that ANF is a covalently crosslinked form of actin. (This work was supported by NIH grant GM32007 and by the Department of Veterans Affairs).

Tu-Pos481

NONLINEAR CAPACITANCE OF THE OUTER HAIR CELL IS INVERSELY RELATED TO LINEAR CAPACITANCE.
((J. Santos-Sacchi and S. Kakehata)) Yale University School of Medicine, New Haven, CT 06510

The outer hair cell (OHC) of the mammalian organ of Corti presents a nonlinear, voltage dependent capacitance which correlates well with the voltage-dependent mechanical activity of the cell. The nonlinear capacitance is believed to reflect the activity of a voltage sensor responsible for gating a molecular motor which resides within the OHC plasma membrane. We have studied the relationship of OHC cell size, which correlates with the location of the cell along the cochlea spiral, and magnitude of nonlinear capacitance. It is demonstrated that the nonlinear capacitance does not decrease in a correlated manner with cell linear capacitance, an indicator of cell length.

OHC capacitance was evaluated with a stair step voltage protocol, under conditions where ionic conductances were blocked (Huang and Santos-Sacchi, Biophysical J. 65, 2228-2236, 1993; Kakehata and Santos-Sacchi, Biophysical J. 68, 2190-2197, 1995). Nonlinear capacitance data were fit with the first derivative of a two state Boltzmann function. Over 150 cells were analyzed and averaged Boltzmann and clamp characteristics were: residual R_s:7.8MΩ, R_m: 155 MΩ. V_h -40.3 mV, C_{lin}:21.29 pF, C_{lin}:20.5 pF, z:0.71. Linear capacitance ranged from about 6 pF to 30 pF. The figure shows capacitance versus voltage plots for two cells, a high frequency basally isolated cell and a low frequency apically isolated cell. The ratios of nonlinear to linear capacitance is 1.7 vs. 1.1, respectively. A regression across all cells evaluated indicates a slope of -0.057, indicating that a decrease in cell linear capacitance is accompanied by a relative increase in nonlinear capacitance. This increase may help to explain the how high frequency OHCs are able to mechanically influence basilar membrane mechanics in the face of reduced receptor potentials caused by the OHC RC time constant at high acoustic frequencies. (Supported by NIDND Grant DC 00273 and DC 02001)

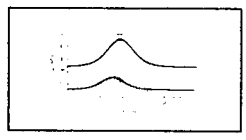

Tu-Pos482

A MODEL FOR GELSOLIN SEVERING OF ACTIN FILAMENTS
L.A. Selden[1], L.C. Gershman[2-4], H.J. Kinosian[4] and J.E. Estes[1,4]
[1] Research and [2] Medical Services, Stratton VA Medical Center, Albany, NY 12208 and Departments of [3] Medicine and [4] Physiology & Cell Biology, Albany Medical College, Albany, NY 12208.

The severing activity of plasma gelsolin appears to be important for shortening of actin filaments (F-actin) which are released into the circulation as a result of tissue injury. Previous studies of gelsolin severing activity have modeled severing as a pseudo-first order irreversible process, however, that model is not consistent with the observation that the apparent severing rate does not extrapolate to zero at zero F-actin concentration. We have modeled gelsolin severing of F-actin as a simple two-step process of reversible binding followed by severing of the F-actin by gelsolin. Severing of F-actin was monitored by the decrease in fluorescence intensity of pyrene-iodoacetamide labeled actin or tetramethyrhodamine-phalloidin bound to F-actin or assayed by the rate of monomeric pyrene-actin addition onto severed filaments. The data indicate that actin filaments are severed rapidly (within ~ 5 sec by 10 nM gelsolin). The association rate constant for gelsolin binding to F-actin was found to be in the range of that expected for a diffusion limited reaction and the K_D for gelsolin binding to F-actin appears to be in the 10 nM range. Increasing the $[Ca^{2+}]$ appears to affect the extent of severing but to have little effect on the observed rate of severing; the $[Ca^{2+}]$ requirement for gelsolin activity decreases at low ionic strength. (Supported by NIH grant GM32007 and by the Department of Veterans Affairs.)

Tu-Pos483

BUNDLING OF LENGTH-REGULATED ACTIN WITH PEG.
((J. Goverman, L. Schick, J. Newman)), Physics Dept., Union College, Schenectady, NY 12308.

Column purified Ca-actin was polymerized in the absence and presence of gelsolin (to regulate mean filament lengths between 50- and 5000-mers) and PEG-8000 (to simulate crowded conditions; 2-8%) using various concentrations of KCl and divalent cations (dc). Bundling was characterized by the scattered light intensity and mean diffusion coefficients obtained from dynamic light scattering, by rheology using an RFSII rheometer, and by visualization using fluorescence and phase contrast microscopy. The minimum [KCl] required for bundling decreases both with increasing [PEG] at a fixed mean filament length, or with decreasing filament length at a fixed [PEG]. In the absence of dc, bundling is reversible on dilution, as determined by intensity levels, diffusion coefficients, and phase contrast microscopy. However, with either 2 mM Mg^{2+} or Ca^{2+} added, bundling is irreversible under conditions of higher [PEG] or longer filaments, indicating that *osmotic pressure effects can not fully explain actin bundling with PEG.* Stiffening the actin filaments with equimolar phalloidin does not affect the conditions or the reversibility of bundling. Experiments with Mg-actin without additional dc showed complete reversibility of bundles, so that weaker dc binding sites appear to be involved in the irreversible bundling. We thank Dr. J. Estes and L. Selden for gelsolin and actin, M. Abessi and Dr. B. Danowski for the microscopy and NSF grant MCB-9316025.

Tu-Pos484

TWO-PHOTON CALCIUM IMAGING OF SINGLE STEREOCILIA IN HAIR CELLS: LOCALIZATION OF TRANSDUCTION CHANNELS AT BOTH ENDS OF TIP LINKS ((Winfried Denk[1], Jeffrey R. Holt[2], Gordon M. G. Shepherd[2], and David P. Corey[2,3])) [1]AT&T Bell Labs, [2]Harvard Medical School

The mechanically gated "transduction" channels in hair cells of the vertebrate inner ear are presumable activated by tension in the tip links, stretching from the tips of shorter to the sides of taller stereocilia. This is consistent with results from several assays, including detection of current flow and focal application of known transduction-channel blockers, which place the channels at the tips of stereocilia. No evidence exists, however, to indicate whether channels are at the upper or lower ends of tip links. We have used the Ca^{++} permeability of the transduction channels as another assay for spatial localization of the channels. Hair cells in the intact sensory epithelium of the bullfrog sacculus were filled with an indicator dye (calcium green 1, CG1) by means of a patch pipet sealed to the cells' basolateral surfaces, and their bundles were deflected with a fluid-jet stimulator. CG1 fluorescence was imaged with a two-photon laser scanning microscope, which limited dye excitation to a plane passing through a hair bundle parallel to a cell's apical surface. Deflection of the bundle increased fluorescence in many but not all stereocilia of a bundle. The fluorescence increase was blocked by depolarization to +40 mV. The number of stereocilia responding to deflection was proportional to the measured transduction current, consistent with Ca^{++} influx through transduction channels as the source of the fluorescence increase. Following a deflection, fluorescence rose first in the tips of stereocilia and then in their bases, consistent with channels at the tips, but in disagreement with previous measurements of Ca^{++} dye fluorescence in hair cells. Some of the shortest stereocilia in a bundle showed a fluorescence increase, as did some of the tallest, indicating that transduction channels can be at either and probably are at both ends of a tip link.

Tu-Pos485

ATPase ACTIVITY OF MYOSIN IN HAIR BUNDLES OF THE BULLFROG'S SACCULUS. ((A. Burlacu, W. D. Tap, and A. J. Hudspeth)) Howard Hughes Medical Institute and Laboratory of Sensory Neuroscience, The Rockefeller University, New York, NY 10021-6399.

Mechanoelectrical transduction by a hair cell of the inner ear displays adaptation: during a protracted deflection of the mechanically sensitive hair bundle, the cell's electrical response decreases over time. It has been proposed that myosin, by moving along the actin cores of the bundle's constituent stereocilia, resets tension in the transduction apparatus and thereby causes adaptation. Previous studies, using photolabeling, immunocytochemistry, and molecular cloning, have supported the existence of myosin Iβ in hair bundles.

We now demonstrate that hair bundles isolated from the bullfrog's sacculus have both K^+-EDTA and actin-activated ATPase activity. Separation of ^{32}P-labeled inorganic phosphate from unreacted [γ-^{32}P]ATP by thin-layer chromatography, followed by quantitation through scanning of phosphor storage plates, enabled us to measure the liberation of as little as 2.5 pmol of phosphate. Because the actin-activated ATPase activity of hair bundles was inhibited by competition with *N*-ethylmaleimide-treated subfragment 1 from myosin II (S1-NEM), myosin ATPase activity could be resolved from that of other bundle ATPases.

The K^+-activated EDTA ATPase activity of the hair bundles from a sacculus was 0.4 ± 0.2 fmol·s^{-1} (mean ± standard deviation). The actin-activated ATPase activity increased from 0.8 ± 0.4 fmol·s^{-1} in 1 mM EGTA to 1.9 ± 0.7 fmol·s^{-1} in 10 μM Ca^{2+}. Addition of calmodulin, at concentrations up to 10 μM, did not affect the myosin ATPase activity.

The results, which indicate that hair bundles contain functional, Ca^{2+}-sensitive myosin molecules, are consistent with the observed role of Ca^{2+} in adaptation and with the hypothesis that myosin forms the hair cell's adaptation motor.

This research was supported by NIH grant DC00241.

Tu-Pos486

PAPAIN ALTERS THE RESONANT FREQUENCY OF FROG SACCULAR HAIR CELLS ((C.E. Armstrong and W.M. Roberts))
Inst. of Neuroscience, Univ. of Oregon, Eugene, OR 97401.

The membrane potential of many auditory and vestibular hair cells undergoes damped sinusoidal oscillations in response to injected current steps. This electrical resonance is thought to contribute to the frequency selectivity of these organs. In the sacculus of *Rana pipiens* there are important discrepancies between biophysical studies of isolated hair cells and studies using more intact preparations. We report here that some of this discrepancy may be attributable to the effects of the enzyme (papain 5125, Calbiochem) used in the isolation procedure. In whole-cell current clamp recording from a semi-intact epithelial preparations, hair cells resonated at frequencies between 30 and 110Hz in response to small depolarizing steps from the resting potential (66±21Hz, mean±S.D., n=19, Fig D). Exposure of the epithelium to papain (0.25mg/ml for 30 min) raised the resonant frequency to 160-250Hz (193±28Hz, n=25, Fig C). This difference is associated with changes in outward (K^+) currents recorded under voltage-clamp (Figs A&B). In addition, several of the hair cells in the semi-intact preparation produced all-or-none spikes, rather than damped oscillations.

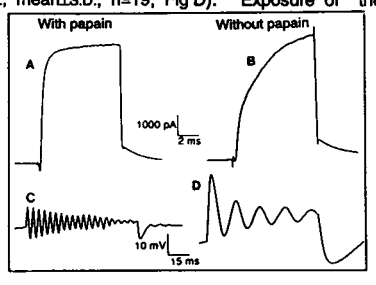

Tu-Pos487

CROSS-LINKING STUDIES OF RADIOLABELLED WILD-TYPE AND MUTANT LARGE MECHANOSENSITIVE ION CHANNEL (MscL) IN *ESCHERICHIA COLI*.

((Claudia C. Häse, Rodney F. Minchin, Alexander C. Le Dain & Boris Martinac)) Department of Pharmacology, Univ of Western Australia, Nedlands, 6709, Australia.

The gene encoding the large conductance mechanosensitive ion channel (MscL) of *E. coli* was recently isolated (Sukharev *et al.*, Nature 368:265, 1994). We have cloned the wild-type and several deletion mutants into the plasmid vector pGEM11Zf(+) under the control of the T7 polymerase promotor. Transformation of these constructs into the *E. coli* strain JM109DE3 carrying an inducible T7 polymerase gene allowed the production and specific labelling of MscL with ^{35}S-methionine. Following induction and labelling of the MscL proteins, a water-soluble or water-insoluble carbodiimide cross-linker was applied to the cells. Treatment with either cross-linker resulted in the appearance of higher molecular weight protein bands corresponding to the size of MscL dimers but no higher order oligomers. However, the majority of labelled protein migrated as a monomer even following carbodiimide treatment, and therefore it appears that the MscL protein predominantly exists in a monomeric form in the *E. coli* membrane with a small portion of molecules existing as dimers. An internal 28 amino acid deletion of MscL did not affect the dimerization, whereas a C-terminal 32 amino acid deletion mutant (kindly provided by P. Blount, University of Wisconsin, Madison, WI) exhibited little or no dimeric form. The observation that the MscL protein is found in a monomeric form in unactivated cells may imply that mechanical stress to the cell membrane is necessary for multimerisation of the MscL protein and consequently channel activation. Further studies, including other types of cross-linkers, in combination with MscL channel activation may reveal which higher order multimers, if any, play a role in channel behavior.

Tu-Pos488

AN N-TERMINAL RECOMBINANT MUTANT OF THE LARGE MECHANOSENSITIVE ION CHANNEL (MscL) OF *ESCHERICHIA COLI* WITH AN ALTERED CONDUCTANCE.

((Claudia C. Häse, Alexander C. Le Dain, & Boris Martinac)) Department of Pharmacology, Univ of Western Australia, Nedlands, 6907, Australia.

We have applied a technique of single-step purification to the large mechanosensitive ion channel (MscL) of *E. coli* by generating a plasmid vector encoding a glutathione S-tranferse (GST)-MscL fusion protein. Proteolytic digestion of the fusion protein by thrombin resulted in the presence of ten amino acid residues at the N-terminus of the recombinant protein that are not found in the wild-type MscL protein. Patch-clamp experiments with this recombinant MscL did not indicate any major effects of these additional amino acids on channel properties (Häse *et al.*, J. Biol. Chem. 270:18329, 1995). In the present study, the *mscL* gene was cloned into this expression system using its unique *NruI* restriction site, resulting in the deletion of part of the N-terminus of the MscL protein. Following thrombin cleavage of this fusion protein the first seven (not including the initial methionine) N-terminal amino acids were deleted but replaced by two different residues, thus resulting in a MscL protein that is five amino acids shorter than wild-type and fifteen amino acids shorter than the recombinant MscL protein. Upon reconstitution into artificial liposomes and examination with the patch-clamp technique, the N-terminal deletion mutant protein formed channel with an altered conductance when compared to both wild-type and the previously examined recombinant MscL. The slope conductance of the wild-type MscL (3.0 nS, Sukharev *et al.*, Biophys J. 65:177) was comparable to the recombinant MscL under our present recording and analysis conditions (2.7 nS), whereas that of the deletion mutant recombinant channels was 2.1 nS. In addition, the N-terminal deletion mutant channels exhibited altered gating kinetics compared to both the wild-type and other recombinant channel. These data suggest that the N-terminus of MscL may play a role in channel pore formation as well as in channel gating.

Tu-Pos489

A MODEL OF THE MODULATORY BEHAVIOUR OF MECHANO-SENSITIVE CHANNELS IN CARDIAC MYOCYTES. ((G. C. L. Bett)) Biophysical Sciences, 120 Cary Hall, SUNY, Buffalo, NY 14214.

There is increasing evidence to suggest that mechanosensitive (MS) channels form part of the mechanoelectric feedback pathway, although the transduction mechanism by which mechanical perturbation of a cardiac myocyte affects its electrical behaviour is unclear. The effect of MS channels on cardiac myocyte activity was explored by use of a computer model. A simple, linear monovalent cation-selective mechanosensitive channel with conductance 25 pS, density 0.3 per μm^2, and various reversal potentials between -15 and -30 mV was incorporated into a mathematical model of an isolated guinea-pig ventricular myocyte. The model was capable of reproducing the changes in action potential shape and duration observed in response to variety of experimental protocols. Even though the MS channel was not permeable to calcium, prolonged opening led to a rise in the intracellular calcium concentration (due to increased calcium window current and altered sodium-calcium-exchange mechanism activity). If the intracellular calcium concentration rose sufficiently, spontaneous calcium-induced-calcium release was initiated from the sarcoplasmic reticulum, and an inward current was generated as calcium was extruded from the cell via the sodium-calcium-exchange mechanism. If the inward current depolarized the cell beyond threshold, extrasystoles were observed. The MS channel model is capable of reproducing many of the experimentally observed effects of stretch. This investigation shows that mechanosensitive channels may be involved in the initiation of stretch-induced arrhythmias, and could provide a valuable site for clinical intervention.

Tu-Pos490

SINGLE-CHANNEL AND WHOLE-CELL STUDIES OF MECHANOSENSITIVE CURRENTS IN CHICK HEART. ((Hai Hu and Frederick Sachs)) Biophysical Sciences, SUNY at Buffalo, NY 14214.

Single channel studies in acutely isolated chick heart cells revealed two types of stretch activated ion channels (Figure 1). One type was a non-selective cation channel, with a conductance of 21.0 ± 0.9 pS reversing at -2.2 ± 3.7 mV (n=6) in normal saline (trace a and inset A); the other was a K^+-selective channel with a conductance of 90.0 ± 4.7 pS and a reversal potential of -70.0 ± 5.4 mV (n=3, trace b and inset B). Both channels were completely blocked by Gd^{3+} (> 30 μM). The presence of single channel activity in a given preparation was strongly correlated with the presence of whole cell mechanical responses.

Whole-cell mechanosensitive currents were evoked by pressing the side of a second pipette against the cell (Hu and Sachs, Bioph. J. 68:A393). The permeability evoked by direct mechanical stimulation was different from that evoked by hypotonic stress. With a nearly ion-free bath solution (containing only 2 mM $CaCl_2$ and mannitol), any currents are dominated by the outflow of intracellular ions. The response to direct stimulation was an outward current (Figure 2, trace a), indicating that it was carried by cations; whereas, the hypotonically induced current was inward going (trace b), indicating that it was carried by anions. Mechanical stimulation did not affect voltage-gated Na^+ (Figure 3), K^+, or Ca^{2+} currents.

Supported by Am. Heart Associa.-NY Affiliate and NIH (FS), and MDRF of SUNYAB (HH).

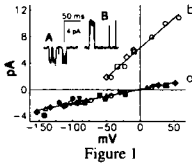

Figure 1

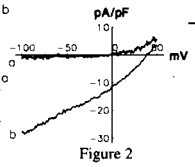

Figure 2

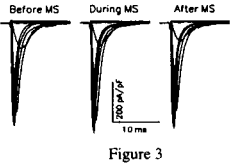

Figure 3

Tu-Pos491

A DEVICE FOR ENCODING ANALOG DATA IN A VIDEO RECORD IN MACHINE READABLE FORM.

((Benyuan Zhang, Tim Heuser and Fred Sachs)) Biophysical Sciences, SUNY, Buffalo, NY 14214.

Contemporary imaging experiments often include the recording of correlated data such as voltages, currents, pressures, etc. The electronic tools available for recording video and analog data are different devices so that establishing the correspondence of particular analog events with particular video frames is awkward, requiring maintenance of time coded pairs of data files. To unify the recordings and allow for automated analysis, we have designed and built a device that encodes the analog data as brightness levels superimposed on the video data. Thus, when a frame is digitized by a frame grabber, the analog data is digitized at the same time.

The device is essentially a video multiplexor. One channel is devoted to video, one to a voltage ramp that provides for internal calibration (particularly necessary when used with video recorders employing AGC), and six to analog inputs. The encoded analog channels appear as a series of vertical stripes at the left of the screen and occupying, in total, about 10% of the screen width. Each stripe represents one of the analog channels. Since the horizontal oscillator is running with a period of ≈ 60 μs, each channel is sampled at ≈15 kHz giving an effective Nyquist bandwidth of ≈7 kHz for each channel. The data is sampled uniformly except for the vertical retrace intervals. The analog system provides subframe resolution at about 500X the frame rate. Amplitude resolution is normally limited by the frame grabber to 8 bits. Nonlinearities and gain changes are corrected by reading the calibration column into a lookup table through which the analog channels are processed.

Supported by MDA and NIH .

Tu-Pos492

***Grammostola Spatulata* Venom Blocks Mechanical Transduction in GH3 Neurons, Xenopus Oocytes and Chick Heart Cells**

((Jeffrey Niggel, Hai Hu, Wade Sigurdson, Charles Bowman and Fred Sachs)) Biophysical Sciences, SUNY, Buffalo, NY 14214. Spon. (R. Spangler)

1) In GH3 cells, hypotonic swelling leads to an elevation of Ca^{2+}. This elevation (sensed with Fura-2) is blocked by *GS* venom at a dilution of 1000X. In contrast, the venom doesn't block the elevation of Ca^{2+} caused by activation of L-type Ca^{2+} channels by high K^+. The venom blocks stretch activated ion channels (SACs) in both cell-attached and outside-out patches. **2)** In *Xenopus* oocytes, venom blocks SACs in cell-attached and outside-out patches. **3)** In acutely isolated chick heart cells, GS venom blocks mechanically activated whole cell currents and SAC currents in cell attached mode. The venom does not affect the inward rectifier or Ca^{2+} currents.

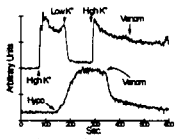

1. Block of hypotonically induced Ca^{2+} uptake (bottom trace) but not depolarization induced Ca^{2+} uptake (top trace).

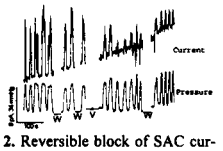

2. Reversible block of SAC currents activated by pipette pressure in an outside-out patch. W=wash, V=venom

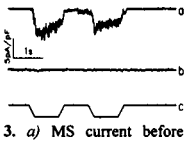

3. *a)* MS current before venom, *b)* after venom (1:1000), *c)* stimulator movement.

Supported by grants from AHA, ARO and SUNYAB to FS.

Tu-Pos493

EFFECTS OF STRETCH ON VENTRICULAR GUINEA PIG CARDIOMYOCYTES HAVING DIFFERENT STIFFNESS ((Cazorla O., Pascarel-Auclerc C., Garnier D. and Le Guennec J-Y.)) Laboratoire de Physiologie Animale, Fac. des Sciences, 37200 TOURS (France)

The Frank-Starling relationship describes the inotropic effect of stretch on cardiac preparations. It is actually admitted that with stretch, the sensitivity for calcium of the troponin C increases. This increase in sensitivity being probably consecutive to a reduced interfilament lattice spacing as sarcomere length (SL) increases. as shown on skinned cardiac prepations[1]. Since we developped a technique to attach and stretch intact cardiac cells[2,3], we described 2 populations of single cardiac cells on the basis of their stiffness[4]. In this study, we tested the behavior of the 2 kinds of cells (stiff and supple) after stretches. We observed that when supple cells were streched, SL and active tension increased, as classically reported. When stiff cells were stretched, we often observed a little or no increase in SL while active tension increased. When we pooled all the data, a good correlation was found only when we plotted active tension vs resting tension while in all the other cases the 2 populations were visible. Therefore, we conclude that resting tension, more than SL, may be an important parameter to modulate active tension.

[1]Wang & Fuchs (1995) J.Mol.Cell.Cardiol., 27, 1235-1244.
[2]Le Guennec et al, (1990) J.Mol.Cell.Cardiol., 22, 1083-1093.
[3]Garnier (1994) Cardiovasc. Res., 28, 1958-1964.
[4]Gannier et al, (1994) Cardiovasc. Res., 28, 1193-1198.

Tu-Pos494

VOLTAGE-ACTIVATED, DIHYDROPYRIDINE(DHP)-SENSITIVE, NON-SPECIFIC CATION CHANNEL IN CILIATED AIRWAY EPITHELIAL CELLS. ((M. L. Woodruff. and E. R. Dirksen)) Dept. of Neurobiol., UCLA Sch. of Med. L.A., CA 90095.

We have previously presented evidence, from Ca^{2+} imaging experiments, that mechanical stimulation of tracheal airway epithelial cells leads to an influx of Ca^{2+} through voltage-activated, DHP-sensitive Ca^{2+}-conducting channels (Boitano, Woodruff and Dirksen, 1995, Am.J.Physiol., in press). In this study we have measured whole cell currents by patch clamping isolated ciliated epithelial cells from rabbit trachea in an attempt to directly assay ionic conducances. With an extracellular solution of (in mM) 40 $BaCl_2$, 100 TEA Cl, 1 $MgCl_2$, 10 HEPES (pH 7.4), 0.1 EGTA and an internal solution of 120 CsMethylsulfonate, 5 EGTA,plus ATP, GTP and an ATP regenerating system we observe a depolarization-dependent outward current between 50 and 200 pA that is reversibly blocked by 1 mM Cd^{2+} and enhanced by DHP agonist BayK 8644 (3 μM). The current is most likely due to Cs^+ efflux since it is observed when Cl^- is removed from the bath (substituting methyl-sulfonate). In addition, inward tail currents indicate that Ba^{2+} can also act as a charge carrier. We suggest that this is a DHP-sensitive, nonspecific cation channel. We are measuring the ion selectivity of this channel and its sensitivity to mechanical stimulation to determine if it maybe the conductance responsible for the Ca^{2+} influx seen in imaging experiments.

This research is supported by the Tobacco Related Disease Research Program of the University of California and NASA Microgravity Research.

Tu-Pos495

CYCLIC STRETCH INDUCED MOLPHOLOGICAL CHANGE INVOLVES PROTEIN TYROSIN PHOSPHORYLATION IN HUMAN UMBILICAL ENDOTHELIALI CELLS.((K. Naruse, and M Sokabe)) Department of Physiology, Nagoya University School of Medicine, Nagoya, Japan 466.

Uniaxial cyclic stretches increased in the level of protein tyrosine phosphorylation in human endothelial cells cultured on elastic silicon membranes. 20 min. The major proteins detected using anti-phosphotyrosine antibodies had molecular masses of approximately 120, 70 and 50 kDa. The tyrosine phosphorylation was inhibited by genistein, a blocker for tyrosine kinases, gadolinium, a blocker for stretch-activated (SA) ion channels, or removal of extracellular Ca^{2+}. Associated with the phosphorylation, *src* and FAK, members of a tyrosine kinase family, were observed to be activated. We have previously reported that stretching endothelial cells caused SA channel-mediated intracellular Ca^{2+}($[Ca^{2+}]_i$) increases (1) and that the cells subjected to uniaxial cyclic stretches showed elongation and alignment of their long axis perpendicularly to the stretch axis. These responses were extracellular Ca^{2+} dependent and inhibited by gadolinium (2). Interestingly the morphological response was found to be completely inhibited by genistein.

Above results suggest that the stretch- and Ca^{2+} dependent protein tyrosine phosphorylation may be necessary for the morphological changes of endothelial cells by uniaxial cyclic stretch.

References
1. K. Naruse, and M. Sokabe, Am. J. Physiol. 264:C1037-C1044, 1993
2. K. Naruse, and M. Sokabe, Biophys. J. 1993

Tu-Pos496

MECHANO-SENSITIVITY OF COLONIC SMOOTH MUSCLE CELLS IN CULTURE.
((S.H. Young, H.S. Ennes, and E.A. Mayer)) CURE: Neuroenteric Biology Group, and Dept. Physiology, UCLA, Los Angeles, CA 90024.

Cultured colonic smooth muscle cells of the rabbit respond to light mechanical deformation of the plasma membrane with a localized increase in intracellular calcium which then spreads wave-like throughout the cell, and then as an intercellular wave into adjacent cells. This response is not blocked by the addition of 100 μM gadolinium chloride, 100 μM lanthanum chloride, or the removal of calcium ions (with addition of 1 mM EGTA) from external saline, indicating that the source of calcium for the response is from intracellular stores. The mechanotransduction is not blocked by treatment with 1 μM thapsigargin, 50 μM ryanodine, 10 mM caffeine, 1μM calphostin C, 50 μM AACOCF$_3$, 1μM U-73122, or 20 μM colchicine. However, the *intercellular wave* is blocked by 1 μM U-73122, and exhibits a propagation threshold of calcium concentration similar to maxima of the inositol 1,4,5-triphosphate receptor (InsP$_3$) vs calcium response curve, and travels through non-responsive cells. Results suggest that mechanotransduction in colonic smooth muscle cells results from a direct mechanical connection between the plasma membrane and internal calcium stores; and that the intercellular calcium wave is mediated by diffusion of a calcium mobilizing messenger molecule, most likely InsP$_3$.
Supported by NIH Grant DK 40919-06

Tu-Pos497

MECHANOSENSITIVITY OF Na$^+$,K$^+$-ATPASE ALPHA SUBUNIT EXPRESSION IN AORTIC SMOOTH MUSCLE CELLS.
((X. Liu, L.J. Hymel, and E. Songu-Mize)) Louisiana State University Medical Center and Tulane University School of Medicine, New Orleans, LA 70112.

We have previously demonstrated that vascular Na-pump activity is stimulated in several rat models of hypertension. To test the effect of sustained cyclic stretch-relaxation stimuli on the expression of α_1 and α_2 subunits of the Na$^+$,K$^+$-ATPase in vascular smooth muscle cells, we utilized the Flexercell Strain Unit to stretch rat aortic smooth muscle cells for several days on a collagen-coated silicone elastomer substratum. Six-second cycles of stretch-relaxation were applied to obtain a maximum of 22% surface elongation (average of 10%) for 4 days. Control cells were not stretched but were grown on a similar surface. The effect of Gd^{3+}, a blocker of stretch-activated channels, was also investigated. At the end of 4 days, protein expression of α_1 and α_2 subunits was determined using Western Blot analysis. Intensity of the bands for α_1 and α_2 was quantified using a computerized image analyzer. In the stretched cells, both the α_1 and α_2 subunit protein band intensities were significantly increased by about 50% compared to those of the nonstretched cells. Treatment with 50 μM Gd^{3+} during the application of stretch prevented the upregulation of α_2 expression, but not that of α_1 expression. Sodium pump activity, determined as ouabain-sensitive $^{86}Rb^+$ influx, was inhibited by stretch; Gd^{3+} had no effect on this parameter. Our results suggest that, in vascular smooth muscle, stretch may be a signal for the upregulation of both the α_1 and α_2 isoforms. However, a differential response of the two isoforms to the blocker of stretch-activated channels implies involvement of different mechanisms. This alteration in protein expression is not reflected in the function of the enzyme.

Tu-Pos498

STRETCH-ACTIVATED NONSPECIFIC CATION AND STRETCH-ACTIVATED Ca^{++} CHANNELS IN RAT MESANGIAL CELLS ADAPT DIFFERENTLY.
((V. Chen, C. Shuman, W.L. Green)), Brooklyn Veterans Affairs Medical Center and SUNY Downstate Medical Center, Brooklyn, New York

Two types of stretch-activated channels have been reported in the membrane of mesangial cells in rat kidneys. One is a 71pS non-selective monovalent cation-permeable channel (capable of carrying Na^+ and K^+). The other is a 21pS Ca^{++} channel, with Ba^{++} as the permeable ion. The adaptation characteristic has not been extensively examined for either channel. As shown by Hamill et al. (1993, 1995), if a stretch-activated ion channel is over-stretched, the adaptation capability of the channel is usually lost. We find that the nonspecific cation stretch channel can adapt only if the constant level of applied stretch is kept sufficiently low. Otherwise, bursts of channel openings continue past the completion of a constant stretch pulse stimulus (30 sec.). However, the Ca^{++} channel adapts quickly--channel bursts stop before the completion of the stretch pulse. Use of Co^{++} to produce open-channel block here with Ba^{++} as the permeant ion yields little adaptation. As the cell attempts to keep cytoplasmic Ca^{++} low by extensive buffering it would be expected that any process bringing Ca^{++} in must be shut off quickly and be limited to very important signals. However, the duration of Na^+ and K^+ entry in a stretch-activated channel can be tolerated somewhat longer, these ions not being as reactive as Ca^{++}. Na^+ entry may activate genes such as c-fos in the nucleus.

Tu-Pos499

ROLE OF INTRACELLULAR MACROMOLECULAR CROWDING AS VOLUME SENSOR IN BARNACLE MUSCLE CELLS.
((J.C. Summers, R. Lajvardi, R. Buechler, H. Chang, C. Peña-Rasgado, Ajaga, S. and H. Rasgado-Flores)) Dept. Physiol. & Biophys. FUHS/Chicago Medical School. N. Chicago, IL 60064

Animals cells continuously exposed to hyposmotic conditions initially swell but subsequently shrink towards their original volume. This process called regulatory volume decrease (RVD) results from the existence of a feedback loop containing at least two functional elements: a sensor that detects the volume increase, and a sensor-activated effector responsible for restoring the original volume. The objective of this work was to assess the role of a reduction in the intracellular macromolecule concentration as volume sensor under conditions where the ionic strength and membrane stretch were maintained constant. Internally perfused barnacle muscle cells were used as models because these cells readily undergo an extracellular Ca^{2+}-dependent RVD when exposed to hyposmotic conditions. The experimental protocol consisted of assessing the effect on cell volume of isosmotically replacing the intracellular concentration of albumin or polymers (i.e., polyethylene glycol or polyvinyl pyrrolidone) by sucrose. The results show that removal of intracellular (36 mg/ml) albumin or polymer induced a significant ($P<0.05$) volume reduction as compared to cells that were continuously perfused in the presence of the macromolecule (control cells). However, this effect was only observed when the molecular weight of the macromolecule was at least 20 KD. The effect was also inhibited when the cells were either exposed to the presence of the Ca^{2+} channel blocker verapamil (0.1 mM) or to the absence of extracellular Ca^{2+}. This indicates that reduction in the intracellular macromolecule concentration activates Ca^{2+} channels and that an increase in the intracellular Ca^{2+} concentration induces RVD. To test this hypothesis we measured the influx of ^{45}Ca in response to reduction in the macromolecule concentration and found a significant ($P<0.05$) increase in Ca^{2+} influx (~2,500 pmoles/cm^2 sec) with respect to control cells. The activation of Ca^{2+} channels was direct and not due to a membrane depolarization because a reduction in the macromolecule concentration induced Ca^{2+} influx and volume loss in voltage-clamped cells in which the membrane potential was held constant.

Tu-Pos500

DIRECT RELATIONSHIP BETWEEN cAMP LEVELS AND VOLUME REDUCTION IN BARNACLE MUSCLE CELLS.
((S. Markowitz, C. Peña-Rasgado, J. C. Summers, D. Zlatnick and H. Rasgado-Flores)) Dept. Physiol. & Biophys. FUHS/Chicago Medical School. N. Chicago IL 60064.

In barnacle muscle cells, exposure to hyposmotic conditions in the presence of extracellular Ca^{2+} (Ca_o) or removal of Ca_o under isosmotic conditions produces an increase in $[Ca^{2+}]_i$ leading to the loss of intracellular osmolytes and water and therefore, cell volume (Am. J. Physiol. 267:C1319-C1328, 1994). The link between the increase in $[Ca^{2+}]_i$ and volume reduction appears to be an increase in intracellular cAMP. This is supported by two main observations: i) an increase in cAMP produces volume reduction in the presence of a constant submicromolar intracellular $[Ca^{2+}]_i$; and ii) an otherwise effective increase in $[Ca^{2+}]_i$ in promoting volume reduction is inhibited by preventing the cAMP-mediated activation of protein kinase A by the presence of the specific cAMP antagonist RpcAMPS (Am. J. Physiol. 267: C1319-C1328, 1994). The present work was undertaken to test the hypothesis that an isosmotic removal of Ca_o and exposure to hyposmotic conditions in the presence of Ca_o induces cAMP synthesis. Barnacle muscle cells attached to the carapace were incubated in the absence and presence of Ca_o under isosmotic (for 1 hr) and hyposmotic conditions (for 3 additional hrs). Every 10 min cells were cut from the bundle and were rapidly frozen in liquid nitrogen, then freeze-dried and weighed. Subsequently, they were homogenized in trichloroacetic acid and their cAMP levels were determined by radioimmunoassay. Under isosmotic conditions, removal of Ca_o induced a significant ($P<0.05$) simultaneous reduction in volume (10 %) and an increase in cAMP levels (from 170 to 250 nmoles/gr dry wt) as compared to cells which were continuously exposed to the presence of Ca_o. Exposure to hyposmotic conditions in the absence or presence of Ca_o produced a similar cell swelling of 50 %. In the absence of Ca_o, the cells remained swollen and their cAMP levels remained at the basal levels (~ 170 nmoles/gr dry wt). However, if Ca_o was present, the cells underwent a significant volume loss of 50% of the swollen volume and the cAMP levels significantly increased to ~340 nmoles/gr dry wt. Thus, cAMP synthesis accompanies volume reduction.

Tu-Pos501

MEMBRANE VOLTAGE AND TENSION INTERACTIONS IN THE GATING OF THE MECHANO-GATED CATION CHANNEL IN *XENOPUS* OOCYTES
((O.P. Hamill and D.W. McBride, Jr.)) Physiology and Biophysics, UTMB, Galveston, TX 77555.

The mechano-gated (MG) channel in *Xenopus* oocytes shows voltage dependent adaptation in response to sustained mechanical stimulation. Furthermore, a step change in the membrane potential from +100 to -100 mV during a constant pressure stimulation results in a transient increase in the number of open MG channels followed by a decrease (i.e., adaptation) (see Fig. 1D. PNAS, 89: 7462). Mechanical decoupling of the membrane from the underlying cytoskeleton by moderate stimulation results in the loss of both voltage dependent opening and adaptation (see Fig. 2B. ibid). In this study we focus on the voltage dependent aspects of MG channel gating. In the absence of mechanical stimulation, hyperpolarizing voltage steps (from 0 to -100 mV or more negative) result in a delayed activation of the MG channel. The delay is ~10 s at -100 mV and decreases to ~2 s at -300 mV. Also apparent is an increase in opening frequency with hyperpolarization. When the voltage stimulus is maintained for minutes, activity disappears (i.e., adapts) but can be reactivated by stronger hyperpolarization. A pressure step that causes rapid adaptation results in an inhibition of voltage gated activity for ~10 s after the step. Another effect of hyperpolarization is to increase the mechanosensitivity of the channel as measured by pressure-response relations. Following mechanical decoupling of the membrane from the cytoskeleton the above voltage gating of the channel is lost, yet the voltage sensitivity of open channel lifetime is retained. These results may reflect voltage effects either on the membrane or the channel itself. Experiments are under way to discriminate between these possibilities. Supported by NIH and NSF.

Tu-Pos502

HIGH TEMPORAL AND SPATIAL RESOLUTION OF MEMBRANE PATCH MORPHOLOGY DURING PRESSURE AND VOLTAGE STEPS. ((D.W. McBride, Jr. and O.P. Hamill)) Physiology and Biophysics, UTMB, Galveston, TX 77555.

Step changes in pressure with a constant voltage indicate that mechano-gated (MG) channels in *Xenopus* oocytes can turn on with delays of less than 2 ms (see Fig. 3 in TINS, 1993: 341). Similarly, while holding the pressure constant, a step change in the membrane potential from +100 to -100 mV results in a sudden (~ 1 ms) increase in the number of open MG channels. However, when the membrane becomes decoupled from the underlying cytoskeleton, changes occur in responses to both pressure and voltage steps. The latency of turn on becomes significantly longer and the voltage-dependent increase in opening of MG channels does not occur. A possible explanation for these phenomena lies in the mechanics of membrane movement and tension changes accompanying the step changes in stimulation. Conventional videomicroscopy techniques have been used to visualize patch movement over the course of a second or longer and in fact report membrane relaxations with $\tau \sim 1$ s (Biophys. J. 59: 722). However, this slow relaxation is inconsistent with the rapid activation we see. One limitation of video rates is that visualization is fixed at 60 Hz or 16 ms per field, which is inadequate for monitoring sub-ms changes. Although high speed cameras exist, they are extremely expensive (> $100 k). In order to overcome this we have used a gateable image intensifier in conjunction with a high resolution camera (480 by 1100 pixels) to take snap shots of successive events while varying the delay within an event by steps of 50 us. We are currently using this technique to discriminate possible mechanisms of MG channel activation and adaptation. Supported by the NSF and NIH.

Tu-Pos503

ON THE NATURE OF MECHANO-GATED CHANNEL ACTIVITY IN CYTOSKELETON DEFICIENT VESICLES SHED FROM *XENOPUS* OOCYTES. ((Y. Zhang, F. Gao, D.W. McBride, Jr. and O.P. Hamill)) Physiology and Biophysics, UTMB, Galveston, TX 77555.

A general assumption is that stretch-activated mechano-gated (MG) channels seen in many nonsensory cells are gated by changes in membrane tension. However, in many cases it is unclear whether the gating tension is exerted by the underlying cytoskeleton (CSK) or the lipid bilayer. Evidence supporting CSK involvement comes from the observation in *Xenopus* oocytes that decoupling of the membrane from the CSK by patch applied suction removes rapid adaptation and significantly reduces the mechanosensitivity of channel activity. However, the cell-attached patch configuration is less than ideal for analyzing morphological events and structures localized at the very tip of the patch pipette. In order to better examine the role of the CSK we have developed a more amenable system involving CSK deficient vesicles formed from *Xenopus* oocytes. Treatment of stripped oocytes with 25 mM formaldehyde for ~ 1 hour causes extensive blebbing of the plasma membrane. With additional time these blebs bud off to form isolated vesicles ranging in diameter from 1 to 20 microns. The general absence of CSK proteins was confirmed by the lack of labeling by fluorescent and immunological probes for actin, microtubules and intermediate filaments. The vesicles can be easily patch-clamped and show dramatic changes in the gating properties of MG channels. In particular, rapid adaptation is absent, the single channel Boltzmann relation has a reduced slope and is shifted to the right (i.e., higher pressures) and the overall maximal patch current response is significantly reduced. In contrast, single channel conductance and voltage dependent lifetime of MG channels remains unchanged. Supported by the NIH.

Tu-Pos504

TESTING THE PUTATIVE ROLE OF A MECHANO-GATED CHANNEL IN *XENOPUS* OOCYTE MATURATION, FERTILIZATION AND TADPOLE DEVELOPMENT. ((N.C. Wilkinson, D.W. McBride, Jr. and O.P. Hamill)) Physiology and Biophysics, UTMB, Galveston, TX 77555.

Although numerous biophysical studies have been carried out on the mechano-gated (MG) cation channel endogenous to *Xenopus* oocytes, little is understood of the role(s), if any, this channel plays in oocyte biology. In order to investigate potential roles, we have monitored *in vitro* maturation and fertilization of the oocyte as well as development of the tadpole in the absence and presence of the MG channel blockers: gadolinium (100 uM), amiloride (2 mM) and gentamicin (1 mM). The drug concentrations chosen are 4-20 times greater than their IC_{50} for block of the *Xenopus* oocyte MG channel. To induce *in vitro* maturation, stage VI oocytes were incubated with progesterone. Maturation was indicated by loss of pigment in the animal pole which reflects germinal vesicle breakdown and was unaffected by the presence of MG channel blockers. Fertilization was carried out using *in vivo* matured oocytes and sperm and each was incubated for ~ 10 minutes in the appropriate test solution prior to mixing. For each drug condition, over 100 oocytes were tested. None of the MG channel blockers affected sperm motility nor their apparent ability to undergo the acrosome reaction and fuse with the oocyte membrane. The blockers also did not decrease the probability of fertilization which was always >95%. Furthermore, in all cases tadpole development proceeded to the free swimming stage (i.e., stage 44) consistent with a previous report (Develop. Growth and Differ. 33: 437). In conclusion, block of MG channel activity does not prevent the processes of oocyte maturation, fertilization or tadpole development. Supported by NIH.

RESPIRATORY FUNCTION

Tu-Pos505

FAST GEMINATE RECOMBINATION OF O_2 WITH *ASCARIS LUMBRICOIDES* PERIENTERIC HEMOGLOBIN. ((J. A. Ridsdale and M.A. Pereira)). Dept. Physiol. And Biophys., Albert Einstein College of Medicine, Bronx NY 10461. (Spon. by J. Wittenberg).

The nematode *Ascaris lumbricoides* is an intestinal parasite of swine. It has two distinct hemoglobins: one in the body wall and one in the perienteric fluid space. The perienteric hemoglobin has a very high oxygen affinity and a very slow rate of oxygen dissociation. We have examined the fast rebinding kinetics of photolysed O_2 of the octameric *Ascaris* perienteric hemoglobin at room temperature with sub-picosecond temporal resolution. This was done using a laser system which includes dual titanium-sapphire regenerative amplifiers. The high-energy pulsed output of the amplifier was frequency doubled to 418 nm for pump-probe experiments. Results indicate that about 20 percent of the deligated population recombined with a time constant of 250 ps. Another geminate phase with time constant around 25 ns has been reported for perienteric hemoglobins of related *Ascaris sp.* (Gibson et al. (1993) *JBC* 268: 16993). (Compare the 4% geminate recombination with 180 ns time constant in the case of myoglobin - CO). This large fraction of rapid geminate recombination suggests that the escape of O_2 is blocked in this hemoglobin after deligation. There was no apparent power dependence of the short-time bleach (2.7 ps) which is similar to that observed in other heme-proteins. Time-resolved changes in the visible spectrum were also examined using white-light continuum pulses.

Tu-Pos506

EPIFLUORESCENCE MICROSCOPY OF PULMONARY SURFACTANT PROTEIN-A (SP-A) ADSORBED ON TO DIPALMITOYLPHOSPHATIDYLCHOLINE (DPPC) FILMS.
((K.Nag, M.L.F.Ruano*, J.Perez-Gil*, C.Casals* and K.M.W.Keough.)) Dept. of Biochem., Memorial Univ., Newfoundland, Canada & *Dept. Bioqumica y Biologia Mol., Unversidad Complutens, Madrid, Spain.

Pulmonary surfactant a lipid-protein mixture maintains alveolar stability. A glycosylated, 35 Kda, octadecameric, pulmonary surfactant (PS) specific protein SP-A, enhances the biophysical properties of PS lipids. Epifluorescence microscopy of fluorescent Texas-Red® labelled SP-A (R-SP-A) adsorbed on to films of DPPC was performed at the air-saline (150 mM NaCl, 5 mM Tris-HCl, pH- 7.4) interface. Analysis of the fluorescence from R-SP-A in DPPC films showed that the protein inserted mainly in the condensed (gel)/fluid phase boundary of the lipid and also to some degree in the fluid phase, at low surface pressures (π). Some amount of R-SP-A remained associated with the lipid films at high π. Increasing amounts of R-SP-A in the DPPC film hypophase (from 0 to 0.26 μg/ml) decreased the lipids condensed phase domain size and the total amount of that phase, and domain distribution. At a lower pH of 4.5, higher amounts of R-SP-A associated with the lipid gel-fluid phase boundary compared to that seen at the higher pH, indicating possible electrostatic as well as hydrophobic interactions of the protein with the lipid. (Supported by MRC, Canada and DGS & NATO, Spain.)

Tu-Pos507

KINETIC STUDIES OF CONCURRENT DESENSITIZATION AND RESENSITIZATION OF THE RELAXATION RESPONSE TO A BETA$_2$ ADRENORECEPTOR AGONIST IN ISOLATED GUINEA PIG AIRWAYS. ((Istvan Sugar, Daniel E. Wachsman, Jill Kavaler, E. Neil Schachter and Saul Maayani)) Biomathematical Sciences, and Physiology and Biophysics(IS) Departments of Anesthesiology (DEN JK and SM), Pharmacology (SM) and Medicine (ENS), Mount Sinai School of Medicine of the City University of New York, New York NY 10029.

Desensitization of activated ß2 adrenoceptor (BAR) in cells in culture occurs within minutes. By contrast, new BAR agonists utilized for preventing airway obstruction in humans are clinically effective for 6-12 h. We addressed this apparent discrepancy with a study of the kinetics of desensitization and resensitization of the relaxation response to a BAR agonist in isolated guinea pig trachea. In tissues maintained at basal tone (4-6 g), 130 nM isoproterenol (ISO) elicited a monotonic, fast (1-3 min) and reproducible relaxation response which could be maintained for up to 45 min and was completely reversed by 1 µM propranolol. In contrast, in tissues pre-contracted with 1 µM carbachol, the initial relaxation to ISO was followed by a slower (20-30 min) and a partial restoration of muscle tone ("fade"). The fade meets criteria for its classification as homologous desensitization of the relaxation response at the BAR level. A propranolol-sensitive steady state was established within 25-30 min at a level of 16±9% of the calculated non desensitized relaxation response. A stochastic model described adequately the observed data. The model assumes that the tissue consists of interacting units where each unit may exist in three different states. Small changes in the inter-unit interactions may cause qualitative changes in the course of the kinetics. We propose that in the isolated guinea pig trachea desensitization of BAR and the concurrent resensitization are distinct processes whose net result maintains a sustained relaxation response to ISO. If this is true, then the sustained response may explain the long term clinical efficacy of inhaled BAR agonists.

Tu-Pos508

LINE TENSION OF CONDENSED DOMAINS IN INTERFACIAL FILMS OF PULMONARY SURFACTANT. ((B. Korcakova, K.M. Maloney, W.R. Schief, D.W. Grainger, V.Vogel and S.B. Hall)). Oregon Health Sciences U., Portland, OR; California Inst. of Technology, Pasadena, CA; U. Washington, Seattle, WA; Colorado State U., Fort Collins, CO.

Compressed monolayers of pulmonary surfactant reach very high surface pressures during normal exhalation and stabilize small air spaces against collapse. We have previously used epifluorescence microscopy to show that condensed domains appear during compression of surfactant monolayers and grow to occupy 25% of the interface. At surface pressures approaching equilibrium spreading values, however, domains decrease in size, producing a film which is again homogeneous. This emulsification of the domains may be important for the performance of surfactant films during repeated compression in the lung. Boundaries between different phases are sites likely to produce uncontrolled collapse at high pressures and formation of structures which could not subsequently reenter the film. Our studies used preparations of surfactant constituents from which specific components were removed to determine their role in the decrease in domain area. Among all of the components the neutral lipids in particular reduce the line tension of the domains even at low surface pressures. We have also determined the extent to which standard equations for line tension predict the observed reduction in domains at high pressures and agree with the expected composition of the domains.

Tu-Pos509

NITRITE-TREATED CRYSTALS OF THE *LIMULUS* HEMOCYANIN SUBUNIT II. ((Shenping Liu and Karen A. Magnus)). Dept. of Biochemistry, Case Western Reserve University School of Medicine, Cleveland OH 44106 (Spon. by J.A. Harpst)

Hemocyanins are oxygen carrier proteins in some invertebrates. Subunit II of hemocyanin from the horseshoe crab, *Limulus polyphemus*, was treated with sodium nitrite and crystallized. A 2.8A resolution data set was collected. The refined structure of the oxygenated form of this protein was used as the initial model and the nitrite treated structure was refined to final R-value of 0.185. The overall structure of the hemocyanin is essentially the same as oxygenated one but the active site has significant changes. The copper-copper distance is 0.7A shorter than the oxygenated protein which is in turn 1.1A shorter than the deoxygenated one. These results suggest that in this structure the coppers are fully oxidized and that NO is not tightly bound. It also further confirms a previous conclusion that oxygen binding involves oxidation of the dicopper center. Supported by NSF MCB9305250.

Tu-Pos510

CHOLESTEROL MODIFIES THE PROPERTIES OF SPREAD OR ADSORBED SURFACE FILMS OF DIPALMITOYLPHOSPHATIDYLCHOLINE PLUS PULMONARY SURFACTANT PROTEIN SP-B OR SP-C. ((K.M.W. Keough and S. Taneva)) Departments of Biochemistry and Pediatrics, Memorial University of Newfoundland, Newfoundland, Canada A1B 3X9

Surface pressure-area measurements were performed on spread monolayers of dipalmitoylphosphatidylcholine (DPPC) plus SP-B or SP-C in the presence of 8 w% cholesterol (CH). CH reduced the stability of the films of DPPC:CH, SP-B/(DPPC:CH), and SP-C/(DPPC:CH) when they were compressed to $\pi \approx 72$ mN/m, in contrast to films of DPPC, SP-B/DPPC, and SP-C/DPPC which exhibited a relatively slow relaxation from the collapse pressure of 72 mN/m. Dynamic cyclic compression beyond collapse of SP-B/(DPPC:CH) and SP-C/(DPPC:CH) monolayers showed that CH diminished their post-collapse respreading compared to the respreading of the protein/DPPC films without CH. The sterol inhibited the rate of adsorption of aqueous dispersions of DPPC containing 2.5 or 5 w% SP-B or SP-C. Results suggest that CH might be detrimental to the interfacial properties of mixtures of DPPC plus hydrophobic surfactant protein deemed desirable in pulmonary surfactant in situ. (Supported by Medical Research Council of Canada).

Tu-Pos511

FKBP12/RYANODINE RECEPTOR COMPLEX RELATES RYANODINE-SENSITIVE AND RYANODINE-INSENSITIVE "LEAK" CA^{2+} EFFLUX PATHWAYS IN SKELETAL MUSCLE SARCOPLASMIC RETICULUM AND BC_3H1 CELLS. INSIGHTS GAINED WITH NOVEL BASTADINES FROM *IANTHELLA BASTA*. ((Isaac N. Pessah*, Tadeusz F. Molinski*, Trena D. Meloy*, Patty Wong*, Paul D. Allen† and Matthew M. Mack*)) *Departments of Molecular Biosciences and *Chemistry, University of California Davis, CA 95616, and †Department of Anesthesia, Brigham and Women's Hospital, Boston, MA 02147

Bastadins (BST) are used to examine the relationship between ryanodine-sensitive and ryanodine-insensitive Ca^{2+} efflux pathways which co-exist in junctional SR membranes vesicles isolated from rabbit skeletal muscle and differentiated BC_3H1 cells in culture which express the skeletal ryanodine receptor (RyR-1) and FKBP12 proteins. One efflux pathway is sensitive to sequential activation and inhibition by micromolar ryanodine (Ry) and is synonymous with the Ca^{2+}- and caffeine-sensitive release mechanism. Block of ryanodine-sensitive Ca^{2+} channels does not alter steady-state loading capacity of SR vesicles. Inhibition of the SERCA pumps with thapsigargin (200-350 nM) results in a rapid release of accumulated Ca^{2+} from actively loaded SR vesicles and mobilizes the SR Ca^{2+} store of intact BC_3H1 cells, even when ryanodine-sensitive Ca^{2+} channels are fully blocked by Ry. Bastadin 5 (BST 5) alone neither rapidly mobilizes Ca^{2+} in the presence of SERCA pump activity (extravesicular Ca^{2+} ≤100 nM), nor does it inhibit Ca^{2+} efflux unmasked by SERCA pumps inhibition. Significantly, BST5 in combination with blocking concentration of Ry effectively eliminates the ryanodine-insensitive Ca^{2+} "leak" and enhances the steady-state loading capacity of isolated SR vesicles (~2.3-fold). These actions of BSTs occur in the same range of concentrations which enhance the number of high-affinity binding sites for [^{3}H]Ry (EC_{50}'s ~2µM). In intact BC_3H1 cells, BSTs alone are ineffective in eliminating the Ca^{2+} leak unmasked by thapsigargin, but accentuate responses to Ry. The effects of BST at the cellular level are correlated with a significant increase in high-affinity [^{3}H]Ry binding to BC_3H1 membranes. These results taken together strongly suggest that BST, through their modulatory actions on the FKBP12/RyR1 complex, convert ryanodine-insensitive leak states into ryanodine-sensitive channels which recognize [^{3}H]Ry with high affinity. FKBP12, through its interaction with ryanodine receptors, may play a fundamental role in determining the filling state of the SR store in resting muscle and influence the pattern of Ca^{2+} signals in cells responding to agonist stimulation by modulating the leak to channel ratio of the ER/SR membrane.

Tu-Pos512

TOPOLOGICAL MAPPING OF THE MITOCHONDRIAL VDAC CHANNEL USING ANTIPEPTIDE ANTIBODIES. ((S. Stanley, D. D'Arcangelis, C. A. Mannella)) The Wadsworth Center, Empire State Plaza, Albany, NY 12201-0509; Department of Biomedical Sciences, The University at Albany, SUNY.

We are raising antipeptide antibodies against segments of the VDAC polypeptide from Neurospora crassa. Of nine peptides tried, six (corresponding to residues 1-20, 62-78, 131-147, 195-210, 251-268, 272-283) have generated antibodies with characteristics (avidity, specificity) suitable for Western and ELISA experiments to determine accessibility of the respective epitopes in mitochondrial outer membranes. Of these, only 2-3 bind to the membranes well enough to be useful as probes in immuno-electron microscopy. Results so far indicate segments 131-147 and 251-268 are exposed on the cytosolic surface of the outer mitochondrial membrane while 1-20, 62-78 (probably), 195-210, and 272-283 are exposed on the interior surface. Additional topological information will be provided by partial proteolysis experiments using the six antibodies as probes. So far, only segment 1-20 has been shown to be accessible in 2-D crystals of VDAC in an open state. An antibody against a segment (272-283) predicted to be an intramembrane β-strand in the open state reacts with membranes but not crystals, suggesting that closed conformers of VDAC may occur in isolated mitochondria. (Supported by NSF grant MCB 9506113.)

Tu-Pos513

TRIGGERS OF THE MITOCHONDRIAL PERMEABILITY TRANSITION (PT) OPEN PORES OF SEVERAL SIZES. ((Aya Sultan and P.M. Sokolove)) Dept. Pharmacol. & Exp. Ther., Univ. of MD School of Med., Baltimore, MD 21201.

Mitochondria can be induced by a variety of experimental conditions to undergo a PT which is thought to reflect the opening of a pore. Pfeiffer and coworkers [*J. Biol. Chem.* (1995) **270**: 4923] have recently described a method for determining the size of the PT pore based on the ability of polyethylene glycols of different average molecular weights to prevent mitochondrial swelling. We have used this method to ask whether pores induced in isolated liver mitochondria by different triggering agents are all the same size? Our results can be summarized as follows: (1) The pores induced by various triggering agents appear to fall into at least 3 discrete size classes. The smallest pores are opened by Ca^{2+}, phenylarsine oxide, diamide, N-ethylmaleimide, carboxyatractylate, and mastoparan. Palmitoyl coenzyme A, cumene hydroperoxide, and the signal peptide of *Neurospora crassa* cytochrome oxidase subunit IV open a significantly larger pore. Still larger pores are opened by butylated hydroxytoluene (BHT) and by BHT plus trifluoperazine. (2) Pore size is governed by the triggering agent but not by its concentration, the rate of recruitment of mitochondria to the transition, or the presence of agents, *e.g.*, Ca^{2+} or P_i, required to facilitate PT occurrence. (3) Tris (20 mM) decreases the pore size measured for many agents. These observations are consistent with the existence of several pores of differing size or a single pore with multiple substates. [Supported by American Heart Association Grant-in-Aid #94007080.]

Tu-Pos514

REGULATION OF MITOCHONDRIAL PHOSPHOLIPASE A_2 (PLA_2) ACTIVITY BY pH, Ca^{2+}, AND $\Delta\Psi$: RELATIONSHIP TO CYTOSOLIC ENERGY STATUS. K.M. Broekemeier and D.R. Pfeiffer, Dept. of Medical Biochemistry, The Ohio State University, Columbus, Ohio 43210

Using intact mitochondria and endogenous phospholipid as substrate, it was determined that changes in cytosolic energy status that are relayed to the mitochondrial matrix affect PLA_2 activity. For example, a small increase in P_i levels has a significant inhibitory effect. In Ca^{2+}-loaded mitochondria, (80 nmol/mg protein), addition of 5μM P_i caused a 40-50% inhibition, with addition of 20μM P_i resulting in up to 75% inhibition. The mechanism of this inhibition has not yet been determined. Increased extramitochondrial pH affects mitochondrial PLA_2 activity in a manner consistent with that observed with the isolated enzyme. An increase in external pH from 6.7 to 8.1 increased observed activity 2.5 fold. The presence or absence of $\Delta\Psi$ has a dramatic effect on the Ca^{2+} requirement for enzyme activity. In the presence of $\Delta\Psi$, (succinate plus rotenone), there is little to no activity in the absence of exogenous Ca^{2+}. However, the Ca^{2+} dependency disappears in the absence of $\Delta\Psi$ (no substrate, plus CCP, valinomycin, and A23187). Although the enzyme retains a pH dependence, at any pH, the same activity is observed, plus Ca^{2+} or plus EGTA. Thus, mitochondrial PLA_2 activity could be responsive to the cytosolic energy state and may link availability of arachidonic acid for further metabolism to the energy requirements of the cell. (Supported by AHA, Ohio Affiliate and USPHS Grant HL49182)

Tu-Pos515

EXTERNAL ADENINE NUCLEOTIDES REGULATE THE MITOCHONDRIAL Ca^{2+} UNIPORTER (M.L. Litsky and D.R. Pfeiffer) Department of Medical Biochemistry, The Ohio State Univ., Columbus, OH 43210..(Sponsored by James O. Alben)

Based on turnover number and apparent voltage (membrane potential) dependence, the Ca^{2+} uniporter is thought to be a gated channel (see T.E. Gunter and D. R. Pfeiffer (1990) *Am J. Physiol. 258*, C755). Rapid, limited and EGTA-dependent reverse activity of this channel is seen by the present authors as reflecting gating behavior, with the amount of Ca^{2+} (Sr^{2+}) released during an initial rapid phase representing the time required to close the channel. Known modulators of other channels (Mg^{2+}, spermine, ATP) have been found to alter this apparent gating behavior. When Mg^{2+} is present in the medium, closure is rapid, but is slowed by spermine (I_{50} ~ 40 μM) or by removing trace contaminates from the mitochondria. Under conditions where channel closure is slow, external ATP accelerates the process by several fold. The ATP effect is concentration dependent, seen in mitoplasts, and seen in the presence of oligomycin and/or carboxyatractyloside. AMP-PNP is partially effective as a substitute for ATP. ADP, but not AMP, antagonizes the ATP effect. Low ATP/ADP ratios apparently favor an open channel and should, therefore, enhance the transfer of a cytosolic Ca^{2+} signal into the mitochondrial matrix space. This scenario provides for a direct link between cytosolic energy status (ATP/ADP ratios) and regulation of the TCA cycle by Ca^{2+} (supported by USPHS grant HL49182).

Tu-Pos516

ISOLATED HEART MITOCHONDRIA TAKE UP Ca^{2+} VIA THE RAPID UPTAKE MODE. ((L. Buntinas, K.K. Gunter, G.C. Sparagna, S-S. Sheu, and T.E. Gunter)) Univ. of Rochester Dept. of Biophysics, Rochester, NY 14642

Many currently believe that the rate of oxidative phosphorylation is mediated by intramitochondrial free [Ca^{2+}]. The rapid uptake mode is a form of mitochondrial Ca^{2+} uptake that has been observed in rat liver mitochondria. This process may enable a mitochondrion to sequester enough Ca^{2+} from physiological pulses to control the rate of oxidative phosphorylation. Recent experiments indicate that the same mechanism probably exists in heart mitochondria.

Chicken heart mitochondria were isolated and placed in a cuvette along with the calcium indicator fura-2. A fluorescence spectrometer was used to measure calcium pulses created by a miropipette injection system. After subjecting mitochondria to a pulse, the samples were centrifuged and $^{45}Ca^{2+}$ uptake was measured. The measured uptake, when extrapolated to a zero pulse width, yielded a value significantly above zero. Pre-equilibrating the mitochondria with radioactive Ca^{2+}, Ca^{2+} depletion, and chelating agents ruled out a rapid exchange mechanism or Ca^{2+} binding to the outside of the mitochondria as possible explanations. This leaves rapid net Ca^{2+} uptake as the likely explanation. These results agree with similar data from rat liver mitochondria and are strongly indicative of the existence of the rapid mode of calcium uptake in heart mitochondria.

Gunter, T.E., K.K. Gunter, S.-S. Sheu, and C.E. Gavin, "Mitochondrial calcium transport: Physiological and pathological relevance." *Am. J. Physiol.* 267:(Cell Vol. 36) C313-C339 (1994)

Sparagna, G.C., K.K. Gunter S-S. Sheu, and T.E. Gunter, "Mitochondrial Calcium uptake from Physiological-type Pulses of Calcium" *J. Biological Chem.* Vol. 270 No.47 in press (1995).

(Supported by NIGMS Grant GM-35550 and NIDA Grant 27334)

Tu-Pos517

OLIGOMYCIN AND DICYCLOHEXYL-CARBODIIMIDE (DCCD) INDUCE CONFORMATIONAL CHANGES IN OSCP IN COMPLEXES RECONSTITUTED WITH OSCP-DEPLETED F_1F_O AND OSCP.
((Ranjana Paliwal and Saroj Joshi)) Boston Biomedical Research Institute and Harvard Medical School, Boston, MA 02114.

The ATP synthesis and ATP hydrolysis activities of mitochondrial ATP synthase (F_1F_O) are inhibited by F_O-inhibitory ligands oligomycin and DCCD. The binding site(s) of these inhibitors is at the DCCD-binding protein which is part of the F_O segment. It is believed that oligomycin and DCCD effect the inhibition by producing a conformational change in F_O that is transmitted to F_1, resulting in impaired binding of the substrate(s) at the catalytic site(s). The oligomycin conferring protein (OSCP), a subunit of mitochondrial ATP synthase, is known to be essential for inhibiting the catalytic activities of the enzyme by oligomycin and DCCD. In order to explore whether OSCP plays a part in propagating inhibitor-induced conformational changes, complexes formed of OSCP-depleted F_1F_O and fluorescence probe derivatives of OSCP mutants were incubated with oligomycin or DCCD. The OSCP variants used were the WT form that contains a unique cysteine at position 118, or genetically engineered double mutant forms wherein the native C118 was replaced by alanine and a new cysteine was incorporated at position 12, 35, 63, 83, 110, 152 or 183. Our data show that emission maximum for acrylodan-labeled mutant form C118A;S183C experienced a specific 2 to 3 nm blue shift following the addition of oligomycin or DCCD to reconstituted complexes. We conclude that S183 region of OSCP is involved in interactions of this subunit with F_O, and in transmitting any putative conformational changes induced by F_O inhibitory ligands. Our data further emphasize the significance of our previously published results relating involvement of amino acids 181-190 of OSCP in mitochondrial energy coupling (Joshi et al (1992) JBC 267, 12860). Supported by NIH GM26420 and AHA 91-1485.

Tu-Pos518

Mg^{2+} AND Ca^{2+} DEPENDENCE OF SUBSTRATE OXIDATION AND OXIDATIVE PHOSPHORYLATION OF ISOLATED RAT LIVER MITOCHONDRIA.

((A. Panov and A. Scarpa)) Case Western Reserve University, Cleveland, OH 44106-4970

The significance of Mg^{2+} and Ca^{2+} in the regulation of the mitochondrial dehydrogenases and oxidative phosphorylation was studied in the control (C-RLM) and Ca^{2+} and Mg^{2+} depleted rat liver mitochondria (MD-RLM). C-RLM were isolated in the presence of 1 mM EGTA. MD-RLM were obtained by incubation of C-RLM with 0.5 μM A23187 + 5 mM EDTA followed by washing in the absence of the ionophore. As determined by atomic absorption spectrophotometry C-RLM contained: Mg^{2+} 15.4 nmol/mg, Ca^{2+} 3.8 nmol/mg RLM; MD-RLM contained: Mg^{2+} 3.5 nmol/mg; Ca^{2+} 2.3 nmol/mg RLM. The rates of oxidation of various substrates in different metabolic states by the MD-RLM are presented in the Table. The corresponding rates for the C-RLM were taken as 100%. Mg^{2+} content in

SUBSTRATE	State 4	State 3	State 3U
Succinate 10 mM + Rotenone	145%	57.8%	72.8%
Glutamate 20 mM, Malate 2 mM	91.3%	38.2%	52.0%
α-Ketoglutarate 10 mM, Malate 2 mM	14.2%	7.7%	19.0%
Pyruvate 1 mM, Malate 2 mM	29.4%	23.2%	25.5%
Acetyl-Carnitine 1 mM, Malate 2 mM	37.0%	40.0%	25.%

the MD-RLM could be restored upon incubation in the sucrose medium at various external $[Mg^{2+}]$. Under the same conditions deenergized MD-RLM accumulate more Mg^{2+} than the energized ones. With succinate and glutamate+malate as substrates, MD-RLM generate 10% higher values of $\Delta\Psi$ (measured with TPP^{+} electrode) than C-RLM. The redox state of the mitochondrial NAD(P)H was also higher with these substrates. The data show that succinate oxidation is very sensitive to the mitochondrial Mg^{2+} content, whereas the oxida- tion of other substrates depends on the presence of both Mg^{2+} and Ca^{2+}. The data obtained propose that besides their effects on mitochondrial ATPsynthase and dehydrogenases, Mg^{2+} and/or Ca^{2+} also control the H^{+} permeability of the inner mitochondrial membrane. (Supported by NIH HL 18708).

Tu-Pos519

EFFECTS OF MUTATIONS AT TWO NEIGHBORING ASPARTATE RESIDUES IN THE L3 LOOP OF E. COLI OMPC PORIN.

((Nazhen Liu, Michael J. Benedik and Anne H. Delcour)) Depts. of Biology and of Biochem. & Biophys. Sciences, University of Houston, Houston, TX 77204.

OmpC porin is one of the most abundant ion channels in the outer membrane of the bacterium *E. coli*. In patch-clamp studies of outer membrane fractions reconsituted into liposomes, porins show a highly cooperative behavior, with long open times interspersed by closures of one or many channels. This gating kinetics has been shown to be voltage-dependent and modulated by a variety of compounds. OmpC is highly homologous to the OmpF porin, whose three-dimensonal structure is known from X-ray studies. The channel is a β-barrel whose pore is constricted by the extracellular L3 loop. L3 is the most conserved loop between OmpC and OmpF and contains many identical charged amino acids, whose roles might be important in gating. In an effort to gain some insight into the relationship between molecular architecture and gating properties, we have introduced a mutation at two separate aspartate residues located on the L3 loop. Using site-directed mutagenesis, we mutated aspartate residues at positions 105 and 118 to uncharged glutamine, and expressed wild-type or mutant genes in porin-deficient cells from an inducible plasmid under *lacZ* promotor control. The D118Q mutation lead to significant changes in both channel conductance and gating kinetics, while the D105Q produced a much milder effect. We postulate that the disruption of salt bridges between Asp118 and arginine residues on on either the barrel wall or the L4 loop confers more flexibility to the L3 loop, resulting in an enhanced gating activity. Supported by NIH grant AI34905.

Tu-Pos520

STRUCTURE FUNCTION RELATIONSHIP IN THE GATING OF OMPC MUTANT PORIN CHANNELS (W56C).

((Mobasheri, H. and Lea, E.J.A.)) School of Biological Sciences, University of East Anglia, Norwich NR4 7TJ, UK.

OmpC porin channels situated in the outer membrane of Gram-negative bacteria have evolved with a high resistance to proteolytic enzymes and natural surfactants, functioning as trimer channels, each monomer of which is approximately 37kD with a exclusion limit of 600 Da .The mutant studied here, was prepared by oligonucleotide directed mutagenesis [N.D. Bishop Ph.D. thesis UEA 1995] of a residue (Trp 56 in OmpC) highly conserved throughout the family of bacterial porins. Reconstituted in a BLM, OmpC wild type channels need a pd of approximately 250 mV for closure. The mutant channel closes at pd's less than 150 mV and exhibits gating at voltages as low as +8 mV (**A**). The single channel conductance in 1M NaCl is 400 ±20 pS (n=30) (see all points histogram of a 120s recording at 140 mV, **B**) compared with 512 pS for the wild type and 614-690 pS for the Dex mutants [Lakey *et al*, FEBS Lett 278, 31-34, 1991]. Asymmetrical channel closure by application of small pd's has been observed at pH 6.5. By PAGE following heat treatment in SDS, it has been shown that the mutant is less stable than the wild type. The substitution of the hydrophobic amino acid (Trp) with (Cys) should decrease the hydrophobic forces by which the monomers are held together causing an inward folding of the barrel wall into the lumen producing smaller conductance. Further, consequent rearrangement of the charged amino acids may result in lower thermal stability and increased the tendency to close at lower pd.

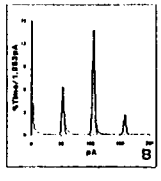

Tu-Pos521

ARCHEAL PORIN-LIKE CHANNELS IN THE ARCHEBACTERIUM *HALOFERAX VOLCANII*.

((M. Besnard*, B. Martinac# and A. Ghazi*)) URA CNRS 1116*, Université Paris-Sud, 91405 Orsay, France, Department of Pharmacology#, University of Western Australia, Nedlands, WA 6907, Australia#

The existence of ion channels in cell membranes of various organisms belonging to two of the three domains of the universal phylogenetic tree, namely Eucarya and Bacteria has been well documented. Here we report a finding of ion channel activities in the membrane of *H. volcanii*, a microorganism belonging to Archea, the third domain of the phylogenetic tree. The archeal membrane vesicles were reconstituted in giant liposomes and examined by the patch-clamp technique or they were fused into planar lipid bilayers. Independently of the technique used the most predominant channel activity encountered exhibited the following characteristics. Channels were open at all voltages in the range beween approximately -120 and +120 mV and exhibited frequent fast transitions to closing levels of different amplitudes. At voltages larger than +/- 120 mV the channels tended to close in a manner characterized by large and slow transitions of variable amplitude. This tendency to close at high membrane potentials was much stronger at one polarity. In general, the channel gating kinetics was complex by showing a whole range of subconductances of various durations in the range 10-300 pS in symmetric 100 mM KCl. At present we do not know how many different types of porin-like channels with above properties may be present in the cell membrane of *H. volcanii*. However, based on their selectivity for chloride or potassium, some channels exhibited preference for K+, whereas the others preferred Cl- with selectivity ratios of approx. 4:1. This suggests that there are at least two types of porin-like channels in these membranes. The above electrophysiological characteristics can be found in bacterial and mitochondrial porins, as well as in eucaryotic maxi-chloride channels. Therefore, the archeal channels may belong to the general class of porin channels.

Supported by Australian Research Council Grant A19332733, CNRS, and a grant to B. Martinac by the French Ministry of Higher Education and Research.

Tu-Pos522

DESIGN AND SYNTHESIS OF A PROTEIN .MAQUETTE THAT BINDS BACTERIOCHLOROPHYLLS

((R. W. Visschers, F. Rabanal, C. C. Moser and P. L. Dutton)). The Johnson Foundation, Department of Biochem. & Biophys., University of Pennsylvania, Philadelphia, PA 19104.

The similarity between the four helix bundle, designed to incorporate hemes [1] and the atomic structure that has recently become available for the peripheral light-harvesting complex from *Rps. acidophila* [2] has motivated us to create a maquette for the Bchl binding site of photosynthetic proteins. In a first effort we have used sequence comparisons from many light-harvesting and reaction center complexes to extract a strucural motif for such binding site. This motif was incorporated into the synthetic four helix bundle protein, replacing one of the original heme binding sites. We will present results that bear on the incorporation of bacteriochlorophylls and other hydrophobic porphyrin derivatives into this maquette.

[1] Robertson D. E.; Farid, R.; Moser, C. C.; Urbauer, J. L.; Mulholland, S. E.; Pidikiti, R.; Lear, J. D. Wand, A. J.; DeGrado, W. F.; Dutton, P. L. (1994) *Nature*, 368, 425-32.

[2] McDermott, G.; Prince, A. A.; Freer, A. A.; Hawthorntwaite-Lawless, A. M.; Papiz, M. Z.; Cogdell, R. J.; Isaacs, N. W., (1995) *Nature*, 374, 517-21

Tu-Pos523

CYTOCHROME OXIDASE: OXYGEN INTERMEDIATES AT STEADY-STATE BY TIME RESOLVED SPECTROPHOTOMETRY. ((M.Brunori, E.D'Itri, A.Giuffrè F.Nicoletti and P.Sarti)) Dep. Biochem. Sciences, University of Rome "La Sapienza", Rome, and Institute of Biol. Chem., University of Cagliari, Cagliari, Italy.

In the reaction of cytochrome oxidase with oxygen two of the optically detectable intermediates identified by transient kinetic methods are the peroxy and the ferryl species. Electron transfer to these intermediates leading to the oxidized state of the binuclear center is functionally important, being correlated to the "stroke" of the proton pump. Nevertheless evidence for the existence of these intermediates at steady-state and their population is lacking.

We have investigated the reaction of cytochrome oxidase at steady-state both in detergent solution and in the reconstituted system by time resolved spectrophotometry combined with singular value decomposition. The results allow to detect at steady-state the presence of a finite population of the ferryl intermediate; however some ambiguity remains about the detection and the contribution of the peroxy intermediate. Approach of the ferryl intermediate to its steady-state occupancy is faster when i) the reducing power is increased, ii) pH is decreased and iii) the electrochemical gradient is collapsed. Quantitation of the absolute value of the population of the peroxy and ferryl intermediates will be of great significance for the mechanism of coupling between electron transfer and proton translocation in cytochrome oxidase.

Tu-Pos524

SITE-DIRECTED MUTAGENESIS STUDY OF SUBUNIT II OF CYTCHROME C OXIDASE ((Yuejun Zhen, John Fetter, and Shelagh Ferguson-Miller)). Dept. of Biochemistry, Michigan State University, East Lansing, MI. 48824

Considerable evidence indicates that CuA is the most kinetically efficient electron entry point for electrons into cytochrome *c* oxidase, and its involvement in proton pumping has also been proposed. Its structure, however, has been the subject of controversy for a long time. The now-available crystal structures show there are two copper rather than one copper ion in the site. We have constructed a site-directed mutagenesis system for subunit II of cytochrome *c* oxidase from *Rhoodobacter sphaeroides* to study the function of this site in the intact enzyme. So far several mutants were made: C256S, H260N, H217C, H260C and M263L, which are all CuA ligands and D214N, a high conserved residue close to the Cu_A site. Among all these mutants, D214N, H260N and M263L were successfully purified. EPR spectra of H260N shows the CuA site is gone and in fact, no copper is present. M263L and D214N have an altered Cu_A site. Oxygen consumption measurements show H260N and M263L have about 1% and 10% of wildtype activity respectively, which indicates an alternative slow electron transfer pathway possibly through heme *a* instead of through CuA and a distorted CuA site can still be capable of electron transfer. Further analysis of these mutants will focus on the kinetics of electron transfer events .

Tu-Pos525

EPR STUDY OF NO COMPLEXES OF *BD*-TYPE UBIQUINOL OXIDASE FROM *ESCHERICHIA COLI*: THE PROXIMAL AXIAL LIGAND OF HEME *D* IS A NITROGENOUS AMINO ACID RESIDUE. ((H. Hori[a], M. Tsubaki[b], T. Mogi and Y. Anraku)) Dept. of Biol. Sci., Grad. Sch. of Science, Univ. of Tokyo, Hongo, Bunkyo-ku, Tokyo 113, [a]Osaka Univ, Osaka 560, and [b]Himeji Inst. of Tech., Hyogo 678-12, Japan

The axial ligands of *bd*-type ubiquinol oxidase were studied by EPR and optical spectroscopies using NO as a monitoring probe. We found that NO bound to the heme d^{2+} of the air-oxidized and fully reduced enzymes with very high affinity and to the heme $b_{595}{}^{2+}$ of the fully reduced enzyme with low affinity. The NO complex of the reduced enzyme exhibited an axially symmetric g-values with $g_{\perp}$=2.041 and $g_{//}$=1.993 and a clear triplet of triplet superhyperfine structure originating from a nitrogenous proximal ligand *trans* to NO was observed. This species was assigned to the heme d^{2+}-NO complex. Another axially symmetric EPR signals with $g_{//}$=2.108 and $g_{\perp}$=2.020 appeared after prolonged incubation with NO and were attributed to the heme b_{595}-NO complex. Further, our recent results indicate that heme *d* exists in the close proximity to heme b_{595} and forming a binuclear metal center.

Tu-Pos526

INFLUENCE OF BULK pH ON STEADY STATE KINETICS OF CYTOCHROME *c* OXIDASE VESICLES. ((I. Perin and P. Nicholls)) Dept. Biosci., Brock University, St. Catharines, ON, Canada L2S 3A1.

Mitochondrial cytochrome *c* oxidase and its bacterial homologs catalyze electron transfer and H^+ translocation across a membrane. These enzymes are highly sensitive to both pH and ionic strength. What are the relationships between redox reactions and proton movement? Are all pH effects upon the enzyme associated with proton movements to and from the binuclear centre? The effect of bulk pH on the biphasic cytochrome *c* oxidase steady-state kinetics in proteoliposomes was investigated polarographically at varying [cyt. *c*]. In 64mM K^+ 100mM HEPES the major pH effect is upon the low affinity V_{max}. This is also the parameter most sensitive to valinomycin and nigericin. K_m values at high and low affinity sites, and turnover at the high affinity site, remain approximately constant from pH 6 to 7.8. K_m values at the low affinity site decrease in the presence of ionophores that abolish $\Delta\Psi$ and ΔpH. Respiratory control ratios increase from pH 6.0 to a maximum at pH 7.0, and then decline with further pH increase. Steady state $\Delta\Psi$ and ΔpH, which control COV, are also modulated by bulk pH. Both proton channel pH effects and catalytic centre pH effects may be needed to explain these findings. Supported by Canadian NSERC grant A-0412.

Tu-Pos527

MITOCHONDRIAL OXIDATIVE PHOSPHORYLATION IN STRESSED HAMSTER HEARTS. ((Nicolai M. Doliba, Q. Chang, Natalia M. Doliba, K. Wroblewski, B.H. Natelson, M.D. Osbakken)) University of Pennsylvania, Philadelphia, PA 19104, Veterans Administration Medical Center, East Orange, NJ 07018, and Bristol-Myers Squibb Company, Princeton, NJ 08543

Stress alone is generally not sufficient to produce serious disease, but stress, imposed upon pre-existing disease can contribute to disease progression. To demonstrate the contribution of stress to the progression of a pre-existing disease, supine-cold-immobilization was imposed on young (Y: 2.5 month, necrotic phase with small vessel coronary spasm) and old (O: 5 month, quiescent phase, between processes of necrosis and heart failure) cardiomyopathic hamsters (CMH). Our hypothesis is that changes in mitochondrial (mito) energy processes are involved in enhanced stress-induced pathology. To evaluate this hypothesis in CMH heart, mitochondrial oxidative phosphorylation (State 3 and State 4 respiration rates, respiratory control index (RCI), and ADP/O) using several substrates (α-Ketoglutarate [Keto]; Pyruvate and Malate [Pyr + Mal], Glutamate and Malate [Glut + Mal]) was measured in Y-CMH and O-CMH (stressed [S] and unstressed [US]) and compared to control (CON: S and US). In unstressed CMH and CON, State 3 and 4, RCI, and ADP/O were similar using all substrates (Keto, Pyr + Mal, Glut + Mal). However, in stressed CMH (both Y and O), RCI was decreased when Keto was used as substrate (Y-CMH-S: ↓ 50% compared to CON-US and 43% compared to Y-CMH-US; O-CMH-S ↓ 39% compared to CON and ↓ 7.8% (N.S.) compared to O-CMH-US). In CON, stress did not significantly change any mito parameter using any substrate. These data suggest that heart mito from Y-CMH, i.e., in the necrotic phase of disease, were more susceptible to stress-induced changes in oxidative phosphorylation than CON and O-CMH.

Tu-Pos528

RESPIRATORY FUNCTION OF DIABETIC RAT HEART MITOCHONDRIA. ((Natalia M. Doliba, Nicolai M. Doliba, K. Wroblewski, M.D. Osbakken)) University of Pennsylvania, Philadelphia, PA 19104 and Bristol-Myers Squibb Company, Princeton, NJ 08543

Myocardial damage in diabetes mellitus (DM) may be related to changes in cardiomyocyte mitochondrial (mito) respiratory function and ion transport. To evaluate these hypotheses, State 3 and State 4 respiration, respiration control index (RCI), ADP/O ratio, and rate of oxidative phosphorylation (ROP), and calcium uptake were measured in heart mito from DM rats and compared to control (CON). Streptozotocin (Strep) pancreatic damage was used to produce DM; Group 1 rats were studied 2.5 weeks and Group 2 were studied 4 weeks after Strep (plasma glucose 400-480 mg/dL and 700-750 mg/dL, respectively). Group 1 showed: 1) decreased State 3, RCI, and ROP with pyruvate plus malate or glutamate plus malate; 2) decreased ROP with α-ketoglutarate; 3) increased State 3, RCI and ROP with succinate; 4) normal ADP/O with all substrates. Group 2 mito showed: 1) greater decrease in oxidation of all substrates than seen in Group 1; 2) decrease in succinate oxidation. $CaCl_2$ was used to stimulate State 3 respiration; Ca^{2+} uptake was recorded by measuring H^+ flux (i.e., $Ca^{2+}/2H^+$ exchange). The first addition of Ca^{2+} ($CaCl_2$ 50 μM) led to increase in $_{o2}$ consumption in CON mito. Two additional doses of $CaCl_2$ (up to 150 μM) were needed to stimulate O_2 consumption in DM mito. The mito calcium capacity did not change in Group 1 and significantly decreased in Group 2. In conclusion, these combined data suggest that the depressed oxidative processes described above may be related to impaired Ca transport in DM mito.

Tu-Pos529

ADENOSINE IMPROVES EFFICIENCY OF CARDIOMYOCYTE RESPIRATION.
((A.M. Babsky, Nicolai M. Doliba, Natalia M. Doliba and M.D. Osbakken)) University of Pennsylvania, Philadelphia, PA 19104 and Bristol-Myers Squibb Company, Princeton, NJ 08543-4000

The influence of adenosine (ADO) on rat cardiomyocyte respiratory function was investigated. Myocytes were prepared using techniques that were previously described (Osbakken e.a.,1992). Oxygen consumption (MVO_2) by cells and mitochondria (Mito) were studied polarographically with a Clark oxygen electrode. Cell concentration in the cuvette was ~3.6 mg protein/ml. A decrease in MVO_2 was observed with the addition of 10^{-5} M ADO to cell cuvette. In this case, the MVO_2 $T_{1/2}$ was 11% longer than in untreated cells. The effects of incubation of cells with 10^{-5} M ADO before cells were added to the cuvette were also studied. After 15 and 30 min of incubation with ADO, the $T_{1/2}$ increased by 15% and 29%, respectively. After 1h of incubation there was a tendency for normalization of respiration rate (closer to that of untreated cells). We propose that the decrease in MVO_2 after ADO exposure may be related to changes in mitochondrial respiratory function. To evaluate this hypothesis, State 3 and State 4 respiration, respiratory control index (RCI) and ADP/O ratio were measured in Mito obtained from cardiomyocytes previously incubated with ADO. Pyruvate (3 mM) + malate (2.5 mM) were used as substrates. Mito from ADO-treated (10^{-5} M, 15 min incubation) cells showed an increase of ADP/O ratio and RCI compared to Mito from ADO-untreated cells. These data suggest that the ADO-induced decrease in cardiomyocyte respiration rate as described above may be related to an increase in efficiency of oxidative phosphorylation, and more economical use of oxygen.

Tu-Pos530

EFFECT OF BRIDGING GROUP LENGTH, BRIDGING GROUP BRANCHING, RING SUBSTITUENTS, AND SELENIUM FOR SULFUR SUBSTITUTION OF THIA(CARBO)CYANINES ON MITOCHONDRIAL NADH OXIDASE ACTIVITY.
((Tarick Abdo and W. Marshall Anderson)) Indiana University Sch. Med., Northwest. Center for Medical Education, Gary, IN 46408

A series of six thia(carbo)cyanines differing in bridging group length, bridging group branching, ring group substitution, and selenium for sulfur substitution were tested for their ability to inhibit mitochondrial NADH oxidase activity at pH 8.0 and 6.5. Bridging group length varied from one carbon (cyanine) to seven carbons (tricarbocyanine); branching included a methyl or ethyl branch in a carbocyanine bridging group; ring group substituents included both methyl and acetate groups. Selenium was substituted for sulfur in a carbocyanine. IC50 for NADH oxidase activity, pH 8.0 was <1μM for the four thiacarbocyanines tested and 5μM for the thiacyanine and ring substituent thiacarbocyanine compounds. The IC50 for NADH oxidase activity, pH 6.5 was also <1μM for three of the thiacarbocyanines including the selenium substituted compound and the methyl branched thiacarbocyanine, 5μM for a tricarbocarbocyanine with propyl side chains, and 40μM for the thiacyanine bridge and ring substituent thiacarbocyanine. None of the compounds inhibited reduction of ferricyanide by NADH, but all significantly inhibited reduction of duroquinone and decylbenzoquinone by NADH at pH 8.0. It is concluded that (1) a three carbon bridge between cyanine groups is necessary for significant inhibition of NADH oxidase activity at pH 6.5 (2) selenium substitution or short branches in the bridging group have little effect on inhibition; (3) ring substitutions diminish inhibitory activity at both pHs.

Tu-Pos531

MYOGLOBIN ENHANCES OXYGEN DELIVERY TO MITOCHONDRIA OF CONTRACTING, ISOLATED HEART CELLS.
((Roy L. White and Beatrice A. Wittenberg)) Temple University School of Medicine, Philadelphia, PA 19140 and Albert Einstein College of Medicine, Bronx, NY 10461.

The steady-state level of mitochondrial NADH is sensitive to the availability of O_2 at the inner mitochondrial membrane when the rates of substrate supply and ATP utilization are constant. When cells are illuminated at 365 nm, the intensity of endogenous cellular fluorescence at 470 nm quantitatively reports mitochondrial NADH. We used fluorescence microscopy to measure NADH in electrically stimulated, individual, isolated heart cells. The mitochondrial pool of NAD becomes fully reduced in the absence of O_2 and fully oxidized at cell death. In control cells with functional myoglobin at high ambient O_2, NADH is reversibly decreased (more oxidized) by about 30% when heart cells are electrically paced at 5 Hz. We report that when cellular myoglobin is specifically inactivated by either sodium nitrite or carbon monoxide, mitochondrial NADH during pacing is significantly elevated compared with control. The reduction of NADH in presence of CO during pacing is further enhanced when glycolysis is blocked by iodoacetate. These data suggest that mitochondria are O_2 limited in the absence of functional myoglobin. In addition, mitochondrial respiration may be regulated down to a lower value in absence of functional myoglobin. We conclude that myoglobin enhances O_2 delivery to mitochondria of contracting heart cells even at high extracellular O_2 pressure.

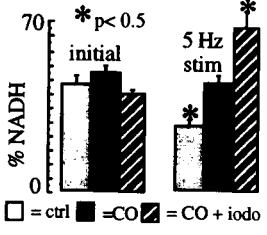

Tu-Pos532

STIMULATION OF MITOCHONDRIAL NADH PRODUCTION IN CARDIAC TRABECULAE VIA PROTOCOLS THAT RAISE CYTOSOLIC [Ca^{2+}].
((Rolf Brandes and Donald M. Bers)) Loyola University Chicago, IL 60153.

We have previously demonstrated, using fluorescence spectroscopy, that mitochondrial [NADH] fell in intact cardiac trabeculae during increased work as assessed by time-averaged isometric force (*F*). The goal of the current study was to investigate the effects of increased average cytosolic [Ca^{2+}] ([Ca^{2+}]$_i$) on the NADH vs. *F* relationship. Figure, A→B, shows the fall of [NADH] while increasing Sarcomere Length (SL) (constant [Ca^{2+}]$_i$) using 1 Hz pacing rate and extracellular [Ca^{2+}] ([Ca^{2+}]$_o$) 0.3 mM. At B, [Ca^{2+}]$_o$ was raised to 2 mM, causing increasing [Ca^{2+}]$_i$ and *F* (+150%) while [NADH] initially decreased along a similar slope as A→B. As steady-state was approached (C→D), *F* was ~constant, while [NADH] rose, suggesting Ca^{2+} stimulation of NADH production. Between D→E, (2 mM) SL was again varied, showing a similar slope as at 0.3 mM (~ -0.2). At constant *F*, stimulation by Ca^{2+} caused a rise of [NADH] (~ 50% offset at B). This protocol was also repeated by controlling [Ca^{2+}]$_i$ via increased pacing rate from 0.25 to 1 Hz at [Ca^{2+}]$_o$ 2 mM, causing a similar 150% rise in *F*, and negative slope. However, the offset was smaller if [Ca^{2+}]$_i$ was raised by pacing than by [Ca^{2+}]$_o$. We conclude that [Ca^{2+}]$_i$ stimulate NADH production and that it depends on how [Ca^{2+}]$_i$ is raised.

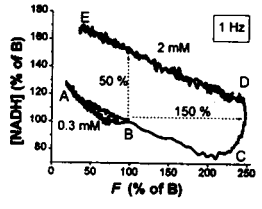

Tu-Pos533

SPATIAL ORGANIZATION OF THE QUINONE ACCEPTOR PART OF MITOCHONDRIAL NADH:UBIQUINONE OXIDOREDUCTASE.
((V.D. Sled, D.S. Burbaev*, V.G. Grivennikova*, I.A. Moroz*, C. Hägerhäll, A.D. Vinogradov*, and T. Ohnishi)) Univ. of Penn., Philadelphia, PA 19104, USA, *Inst. of Chem. Phys., Russian Acad. of Sci., 117977 Moscow, Russia, *Dept. of Biochem., Moscow State Univ., 119899 Moscow, Russia.

Progressive power saturation and temperature dependence of the EPR signals of free radical species have been analyzed in tightly coupled submitochondrial particles. During the steady-state oxidation of NADH or succinate two uncoupler sensitive ubisemiquinones (a fast relaxing SQ_{Nf} and a slow relaxing SQ_{Ns}) are formed in the NADH: ubiquinone oxidoreductase (Complex I) segment of the mitochondrial respiratory chain. The two semiquinone species behave differently in Complex I in the "active" (pulsed) or in the "inactive" (resting) states and exhibit different sensitivity towards rotenone. The distances between Q_{Nf}, Q_{Ns}, and iron-sulfur cluster N2 were estimated from the analysis of EPR spectral and relaxation changes caused by spin-spin interaction. We have also used spin relaxation enhancement effect of dysprosium to determine the distance from the cluster N2 and SQ_{Ns} to the membrane surface. A possible topographical organization of redox centers at the quinone acceptor side of Complex I and its implication on the mechanism of energy coupling in Complex I are discussed. (Supported by NIH Fogarty grant RO3 TW 00140-01A2 (T.O. and A.V.) and by NIH grant GM 30376 (T.O.))

Tu-Pos534

Q_y-EXCITATION RESONANCE RAMAN STUDIES OF PHOTOSYNTHETIC ANTENNA PIGMENTS. ((J. R. Diers[1], R. E. Blankenship[2], and D. F. Bocian[1])) [1]Department of Chemistry, University of California, Riverside, CA 92521, [2]Department of Chemistry and Center for the Study of Early Events in Photosynthesis, Arizona State University, Tempe, AZ 85287. (Spon. by B. Cohen)

Q_y-excitation resonance Raman (RR) spectra have been obtained for films of various bacteriochlorophyll *c*'s (BChl *c*) extracted from light harvesting chlorosomes. Films of the BChl *c* pigments exhibit large red-shifted Q_y absorption bands (as compared to pigment monomers) similar to those observed for the pigments in intact chlorosomes. The RR spectra of the BChl *c* pigments exhibit a unique pattern of low frequency modes. This pattern parallels that observed in femtosecond coherence experiments. The RR spectra serve as benchmarks for interpreting the time-resolved data and aid in understanding the extremely fast energy transfer processes in the chlorosomes of green bacteria.

Tu-Pos535

EVIDENCE FOR LONG RANGE ENERGY MIGRATION IN THE MACROAGGREGATES OF LHCII. ((V. Barzda[1,2], G. Garab[1], V. Gulbinas[2] and L. Valkunas[2])) [1]Institute of Plant Biology, Biological Research Center, Szeged, Hungary; [2]Institute of Physics, Vilnius, Lithuania.

Picosecond transient absorbance kinetics under singlet-singlet annihilation conditions and steady-state spectroscopic features, absorbance, circular dichroism and low temperature fluorescence spectra, were investigated in large, 3-dimensional, stacked lamellar aggregates of the purified light harvesting chlorophyll a/b complexes (LHCII) and its form of small aggregates. Our data show that macroorganizational parameters significantly influence the ultrafast absorbance kinetics as well as the steady state spectroscopic properties of the LHCII aggregates. In small aggregates ($d \approx 100$-200 nm) of trimers the decay kinetics could be described with a model of percolation type of energy migration in a cluster of small number of pigment molecules. In stacked lamellar aggregates ($d \approx 2$-4 μm), which exhibit "anomalous" psi-type spectroscopic features, the absorbance transients were much faster and the kinetics were fully consistent with a model describing singlet-singlet exciton annihilation processes in 3-dimensional (infinitely) large structures. These data suggest that LHCII macroaggregates can constitute a structural basis for long-range migration of the excitation energy.

Tu-Pos536

LIGHT-INDUCED REVERSIBLE CHANGES IN THE CHIRAL MACROORGANIZATION AND IN THE EXCITATION ENERGY DISSIPATION OF THYLAKOID MEMBRANES AND MACROAGGREGATES OF PURIFIED LHCII. ((V. Barzda, A. Istokovics, I. Simidjiev and G. Garab)) Institute of Plant Biology, Biological Research Center, Szeged, Hungary.

By the aid of circular dichroism measurements we show that granal thylakoid membranes undergo light-induced reversible structural changes that, as shown by fluorescence, bring about an increase in the dissipation of the excitation energy. The structural changes, albeit amplified by the transmembrane ΔpH, are shown to be largely independent of the photochemical activity of the membranes. Further, chirally organized, lamellar macroaggregates of the chlorophyll a/b light harvesting complex of photosystem II (LHCII), but not the trimers, also exhibit reversible light-induced structural changes associated with reversible changes in the fluorescence yield. It is proposed that long-range energetic coupling inside densely packed chirally organized lamellar aggregates is responsible for the structural flexibility of the macroaggregates; these structural changes alter the photophysical pathways. This mechanism is likely to be involved in the regulation of the energy dissipation in the antenna.

Tu-Pos537

TIME-RESOLVED PHOTOSYSTEM II CHLOROPHYLL *a* FLUORESCENCE IN BARLEY *CHLORINA* MUTANTS: PHOTOCHEMISTRY, PHOTOPROTECTION AND PHOTOINHIBITION. ((A. M. Gilmore[1], T. L. Hazlett[2], P. G. Debrunner[3] and Govindjee[1])) [1]Dept. Plant Bio., [2]LFD, Physics Dept., [3]Physics Dept., UIUC, Urbana, IL 61801.

Photosystem II (PSII) chlorophyll (Chl) *a* fluorescence lifetimes were measured in barley wild-type and *chlorina* f104 and f2 mutants to determine the effects of the PSII Chl *a+b* antenna size on the de-excitation of absorbed light energy. These barley *chlorina* mutants have drastically reduced contents of PSII light-harvesting complex pigment-proteins and of Chl molecules. PSII Chl *a* fluorescence intensity and lifetime parameters were similar and thus independent of the PSII light-harvesting antenna size at both maximal (at F_0) and minimal (at F_m) PSII photochemistry. Further, the fluorescence intensity and lifetimes, as affected by the trans-thylakoid membrane pH gradient (ΔpH) and the carotenoid pigments of the xanthophyll cycle, were also independent of the antenna size differences. The effects of xanthophyll dependent photoprotective processes on the PSII Chl *a* fluorescence lifetime distributions were consistent with those reported earlier [Gilmore et al. (1995) Proc. Natl. Acad. Sci. USA **92**:2273-2277]. The xanthophyll dependent processes increased the fractional intensity of a Chl *a* fluorescence lifetime distribution centered around 400 ps, at the expense of a 2 ns lifetime distribution. We suggest that the combined effects of the xanthophyll pigments and ΔpH cause structural changes in the pigment-protein complexes of the PSII inner or core antennae; these changes apparently switch the entire PSII unit to an increased rate of heat dissipation resulting in the shorter fluorescence lifetime distribution. In contrast to the xanthophyll-dependent photoprotection, strong light induced photodamage to the PSII reaction center in air (photoinhibition) decreased the lifetime of the 2 ns component with increased time of light exposure. We suggest that photoinhibitory light treatment apparently causes a gradual increase in the rate constant for a non-radiative decay pathway of the charge-separated state in the reaction center that decreases the Chl *a* fluorescence lifetimes. AMG, PGD and G thank NSF/USDA/DOE grant #1-5-28046 for support. TLH thanks NIH grant #RR03155.

Tu-Pos538

FLUORESCENCE FROM LOW-ENERGY CHLOROPHYLLS IN PHOTOSYSTEM I AT 295 K. ((Erin M.Gill*[1] and Bruce Wittmershaus*[2])) [1]Dept. of Physics, Univerisity of Colorado, Boulder, CO 80309 and [2]Div. of Science, Penn State-Erie, The Behrend College, Erie, PA 16563.

Photosystem I (PSI) contains a small number of chlorophylls with a fluorescence maximum far to the red of the absorption peak of the electron donor, P700, of the reaction center. Emission from these low-energy chlorophlls (LE Chls) is easily observed at 77 K where it dominates the fluorescence spectrum at 720 nm. At physiological temperatures, they are not easily identified resulting from their small number, relatively weak fluorescence, and the presence many overlapping bands of fluorescence from other chlorophylls. The function of these LE Chls is unknown. We report fluorescence measurements from a PSII-less mutant of the cyanobacterium *Synechocystis* sp. PCC 6803 at 295 K where emission from LE Chls is resolved. To achieve this, laser excitation of wavelengths from 695 to 720 nm are used to enhance direct excitation of the LE Chls. The problem of observing scattered excitation light is overcome by using a Raman spectrometer. A broad, fluorescence band peaking at 710 nm is observed and attributed to the LE Chls of PSI.

* Work conducted while at the Dept. of Physics and Astronomy, Arizona State University, Tempe, AZ and supported in part by the Center for the Study of Early Events in Photosynthesis and the Arizona State University Laser Facility.

Tu-Pos539

PROTEIN RESPONSE TO Q_A REDUCTION IN WILD TYPE AND EL(L104) *RB. SPHAEROIDES* REACTION CENTERS INVESTIGATED BY LIGHT-INDUCED FTIR DIFFERENCE SPECTROSCOPY
((J. Breton[1], E. Nabedryk[1], J. P. Allen[2], & J. C. Williams[2])) [1]SBE/DBCM, CEA-Saclay, France; [2]Dept Chemistry and Biochemistry, ASU, Tempe, AZ

In reaction centers (RCs) from *Rhodobacter sphaeroides*, Glu L104 is thought to be hydrogen bonded to the 9-keto group on ring V of the bacteriopheophytin electron acceptor (H_A). Light-induced Q_A^-/Q_A FTIR difference spectra of the photoreduction of the primary quinone (Q_A) in RCs from wild type (Wt) and from the EL(L104) mutant in which Glu L104 is replaced by Leu have been measured in ^1H_2O and ^2H_2O. A differential signal, positive at 1730 cm^{-1} and negative at 1724 cm^{-1}, in the ^1H_2O-minus-^2H_2O double-difference spectrum of Wt RCs is absent in the corresponding spectrum of the mutant. This signal is likely to be due to the C=O mode of the protonated carboxylic group of Glu L104 that is downshifted by a few cm^{-1} upon $^1H/^2H$ exchange. The Wt-minus-mutant double-difference spectrum in ^1H_2O shows a complex spectral feature, with a positive peak at 1728 cm^{-1} and negative lobes at 1734 and 1722 cm^{-1} that cannot be interpreted simply in terms of the C=O mode of Glu L104 alone. Another candidate for the signals around 1730 cm^{-1} is the 10a-ester C=O of H_A that is in partial conjugation with ring V and that has been proposed to absorb at 1732 cm^{-1} in the H_A^-/H_A spectra of Wt. In this case, this C=O mode would give a differential signal upon Q_A^- formation and would downshift by ≈ 6 cm^{-1} upon the loss of the hydrogen bond to the 9-keto group in EL(L104). The present FTIR results confirm that Glu L104 is protonated in Wt RCs and show that the reduction of Q_A can induce a pronounced electrostatic effect on molecular vibrations located about 10 Å away from Q_A. ([2]Supported by the NIH)

Tu-Pos540

INTERSUBUNIT PROTEIN-PROTEIN INTERACTIONS AT THE Q_o SITE OF THE bc_1 COMPLEX ((A. Sami Sarıbaş, Mariko Tokito and Fevzi Daldal)) Plant Science Institute, Department of Biology, University of Pennsylvania, Philadelphia. PA 19104.

In *Rhodobacter capsulatus*, bc_1 complex is composed of three catalytic subunits: cyt *b* (44 kD), cyt c_1(33 kD) and FeS protein (24 kD), all required for a functional complex. We have previously reported that the cyt *b* mutants T163F(or P) have no detectable bc_1 complex in their membranes. Among the revertants, second site mutations were identified in cyt *b* (G182S) in FeS protein (A46T) and in cyt c_1(R46C). In all cases, the revertants regained an SH or OH group which was lost by substitution of T163 with F indicating that its substitution by a bulky residue such as F, and the loss of a H bond leads to the disassembly of the bc_1 complex. T163F+B:G182S and T163F+C:R46C revertants exhibited unusually low bc_1 activity (1-4 % of a wild type strain). However, transient kinetics indicated that their single turnover rates were approx. 20 % of that of wild type strain. In contrast, T163F+F:A46T exhibited approx. 20 % of the bc_1 activity, and 60 % of single turnover rates of a wild type strain. T163F+B:G182S and T163F+C:R46C contained substochiometric amounts of FeS protein in comparison to their cognate cyt *b* and c_1 subunits. Further analysis of T163F+B:G182S revealed that in this mutant the FeS protein was cleaved off from the membrane to yield soluble form of 20 kD peptide. The cleavage site appears to be in the vicinity of position 46 of FeS protein, where the suppressor mutation A46T was also found. This suggests that T163F+F:A46T revertant provides a better interaction between the FeS protein and the other subunits by modifying this region. The overall findings indicate that the FeS protein, cyt *b* and cyt c_1 interact with each other in forming the Q_o site of the bc_1 complex. Supported by NIH grant GM 38237.

Tu-Pos541

THE TOPOLOGY OF THE CD HELIX OF THE CYTOCHROME *b* OF THE CYTOCHROME b-c_1 COMPLEX FROM *R. SPHAEROIDES* ((H. Tian, L. Yu, M. W. Mather and C. A. Yu)), Oklahoma State University, Stillwater, OK 74078 (Spon. by R. Burnap)

Previous studies of the cytochrome b-c_1 complex (bc_1) from beef heart have established that one of the Q-binding peptides corresponds to residues #158-171 of cytochrome b of *R. sphaeroides*. This peptide is located in an extra-membrane amphipathic "cd" helix in the eight-transmembrane helix model of cytochrome *b*. To establish that this Q-binding peptide may form part of the Q_o site and to confirm the putative topology of the cd helix, three amino acid residues, S155, S175 and A185, which are located before, within, and after the cd helix, were replaced with cysteines. While mutant S155C cells do not grow photosynthetically, S175C and A185C show the same photosynthetic growth behavior as that of the wild-type or complement strain. Purified S175C and A185C bc_1 complexes have a similar activity and an identical K_m for Q_2H_2 to those of the complement strain. When the purified complexes were treated with N-ethylmalemide (NEM), no change in enzymatic activity was observed with the S175C complex, but a more than 90% activity loss was observed with A185C. This suggests that A185 may be involved in interaction with other segments of cytochrome *b* or its neighboring subunits. When intact chromatophores of the A185C mutant were treated with NEM, no loss of activity was observed. Under the same treatment disrupted chromatophores lost 90% of this activity. This result indicates that A185 is located on the periplasmic side of chromatophore membrane and thus supports the current eight transmembrane model of cytochrome *b*. This work was supported by a grant from NIH (30721).

Tu-Pos542

STRUCTURE-FUNCTION STUDIES ON THE CYTOCHROME b_6f COMPLEX, CYT *f*, AND RIESKE PROTEIN. ((M. Ponomarev, G. Soriano, D. Huang, H. Zhang, C. Carrell, J. L. Smith, and W. A. Cramer)) Dept. of Biol. Sci., Purdue Univ., W. Lafayette IN 47907. (Spon. by L. A. Sherman)

Two interesting features of the high resolution structure of the lumen-side domain of cyt *f* are (i) a basic region at the interface between large and small domains proposed to be a docking site for plastocyanin (Martinez *et al.*, *Structure*, 2, 95-105, 1994), and (ii) a buried internal water chain (Martinez *et al.*, submitted), four H_2O of which extend approx. 12Å from the Nδ1 of the His25 heme ligand toward Lys66 of the basic region. (i) To test the PC docking site, Lys58-Lys 65-Lys 66 were mutagenized to Gln, Ser, and Glu, respectively, in *Chlamydomonas reinhardtii*. This resulted in a large decrease, relative to wild type, in the amplitude of flash-induced cyt *f* oxidation and the slow (msec) $\Delta\psi$ in heterotrophically[1], but not in photoautotrophically, grown cells. (ii) The conserved Q158, N168, and N232 whose side chains H-bond to the buried H_2O, have been mutated to Leu, Phe, and Leu to test the effect of disrupting the H_2O chain. (II) A water-soluble 139 residue fragment of the Rieske protein, with N-terminal sequence NH_2-Phe-Val-Pro-Pro-Gly-Gly-, was isolated from the chloroplast b_6f complex with approximately 100 % [2Fe-2S] content and a normal visible absorbance signal. 3D crystals can be rapidly grown that diffract well, but are at present not single. (III) 3D crystals have been obtained of the cytochrome b_6f complex, isolated as a dimer from the thermophilic cyanobacterium, *M. laminosum*. [Supported by NIH GM-38323 and USDA 9501148; [1]cyt f oxidation rate also decreased by 10-20 fold in double mutants of K187 and any one of K58, 65, or 66 (R. Malkin, J. Fernandez-Velasco, and J. Zhou, *pers. comm.*)].

Tu-Pos543

THE DOCKING OF PLASTOCYANIN WITH CYTOCHROME *f*: A MECHANISM BASED ON THREE PROPOSED COMPLEXES. ((Douglas C. Pearson Jr. and Elizabeth L. Gross)) Department of Biochemistry/Biophysics Program, The Ohio State University, 484 West 12th Avenue, Columbus, OH 43210

Three docking configurations between poplar plastocyanin (PC) and turnip cytochrome *f* (cyt *f*) are proposed based on analysis of the electrostatic properties of the molecular structures and possible hydrophobic interactions and steric interference between the two molecules. Together, these docking configurations provide a hypothesis for the mechanism of docking of PC with cyt *f* leading to electron transfer. The initial attraction between PC and cyt *f* is electrostatic in nature, with negative charges (including residues 42-44, 59-61, and 79) on PC being attracted to positive charges (including residues 58, 65, 66, 187, and 209) on cyt *f*. When the molecules are in a docked configuration, which we call Dock 1, K187 on cyt *f* and D44 on PC are adjacent, as well as K58 on cyt *f* and E59 on PC. These interactions correspond exactly to cross-links observed by Morand et. al. (*Biochemistry* 28:8039); therefore, we propose that Dock 1 represents the structure of the Morand's observed complex. Brownian dynamics simulations give insight into the trajectory by which PC docks with cyt *f* in the Dock 1 complex. We further propose that Dock 1 is a pre-docking complex; that after this interaction is established, PC and cyt *f* fold together, with the hinge being the D44/K187 link, to form a complex where H87 (a ligand to the copper center) on PC is adjacent to Y1 (a ligand to the heme) on cyt *f*. This complex, represented by Dock 2 in this work, is held together by non-polar interactions by residues surrounding H87 and Y1. The hydrophobic interactions can be improved by the breaking of the D44/K187 link, as has been done in Dock 3 in this work, at the cost of increased electrostatic repulsion. We propose that a dock like similar to Docks 2 and 3 is the electron-transfer active dock, and the electrostatic repulsion resulting when H87 is adjacent to the heme is the force that drives PC away from cyt *f* once electron transfer is complete.

Tu-Pos544

SPECIES VARIATION IN THE ELECTROSTATIC FIELD OF PLASTOCYANIN: IMPLICATIONS FOR THE ELECTROSTATIC DOCKING WITH CYTOCHROME *f*. ((Elizabeth L. Gross, William Weily, Douglas C. Pearson Jr., and Michael Farrow)) Dept. of Biochemistry and Biophysics Program, The Ohio State University, 484 W. 12th. Ave. Columbus, OH, 43210.

Initial attraction between cytochrome *f* (cyt *f*) and plastocyanin (PC) is electrostatic in nature. Positively-charged amino acid residues on cytochrome f produce a positive electrostatic field which attracts PC due to the negatively-charged electrostatic field generated by two clusters of negatively-charged residues. In higher plant species such as poplar and spinach, Patch A consists of residues # 42-44 and either residue #79 or 45 and Patch B consists of residues #59-61. Whereas Patch A is highly conserved in Pcs from all higher plants and algae, there is significant variability in patch B. For example, in parsley PC, residues #59 and 60 are absent but another residue (E85) appears in a similar location. To examine the effects of these amino acid changes on the electrostatic field (and hence on docking possibilities), the electrostatic fields for PCs from poplar, french bean, *Chlamydomonas*, *Enteromorpha*, and *Synechocystis* were calculated and displayed using the program GRASP. Docked complexes were formed using HyperChem and GRASP. The structure of *Synechocystis* PC was obtained by homology modeling using the program QUANTA. It was found that the general shape and magnitude of the electrostatic field was conserved for PC from the higher plant and algal species although different residues participated in the different cases. In contrast, the electrostatic field of *Synechocystis* was quite different with a field of positive potential extending over both potential binding sites on PC (H87 and Y83). A large negative field does exist at the end of the molecule opposite H87 but probably is not directly involved in binding. It is proposed that, if there is an electrostatic dock possible between *Synechocystis* PC and the corresponding cyt *f*, it is formed between positive charges on PC and negative charges on cyt *f*.

Tu-Pos545

PARTICIPATION OF D36, D38, D102, D104 AND E161 IN PROTON TRANSLOCATION IN BACTERIORHODOPSIN ((J. Riesle[‡], J. Heberle[#], D. Oesterhelt[‡], N.A. Dencher[§])) [‡]MPI Biochemie, 82152 Martinsried, Germany; [#]KFA, 52425 Jülich, Germany; [§]Technische Hochschule Darmstadt, 64287 Darmstadt, Germany

At present almost no knowledge exists about the functional relevance of the amino acid residues at the cytoplasmic (CP) surface of the light-driven proton pump bacteriorhodopsin (BR) although a prerequisite for efficient vectorial proton translocation by BR is the efficient capture of protons from the alkaline cytoplasm of the cell. To identify residues involved in the elementary proton transfer reaction steps in the CP part of BR, the aspartic and glutamic amino acids D36, D38, D102, D104, and E161 were replaced by cysteine and arginine (i.e., a negatively charged residue by a neutral or positive one at the pH of investigation) and the effect of these replacements on the photo- and transport cycle were examined by visible and infrared spectroscopy, biochemical modification studies, and activity assays in intact cells. Of the five CP amino acids studied, only the replacement of D38 resulted in severe alterations of the reaction steps in BR during the second half of the photocycle. Our data show that D38, which was always considered as a freely accessible CP surface residue lacking any specific functional importance, is an essential part of the CP proton uptake pathway connecting the membrane surface with the Schiff base of BR. It is probably the first amino acid residue at the CP entrance. D38 is involved in the initiation of the late steps in the functional cycle, i.e. occurrence of the intermediates N, O, modulation of the hydrogen-network and of conformational changes in the protein moiety as well as deprotonation/reprotonation of D96. On the other hand, the surface exposed amino acids D36, D102, D104, and E161 seem to efficiently collect protons from the aqueous bulk phase and funnel them to the entrance of the CP proton pathway.

Tu-Pos546

Photo-Induced Electron Transfer between Nucleosides and Nucleotides complexed with Tetrakis(4methylpyridyl)porphine. ((R. Jasuja[1], D. M. Jameson[2], C. K. Nishijo[1] and R. W. Larsen[1]).[1] Department of Chemistry, [2] Department of Biochemistry and Biophysics,University of Hawaii at Manoa, Honolulu, HI-96822.

The singlet excited state of Tetrakis(4-*N*-methylpyridyl)porphine (T4MPyP) interacts very differently with the four mononucleotides and mononucleosides of DNA in aqueous solution. Addition of the nucleotides of adenine, thymine or cytosine to a solution containing T4MPyP results in an increase in the fluorescence intensity of the porphyrin while addition of guanine quenches the intensity substantially. Optical absorption measurements demonstrate non-covalent binding of the nucleotides with the porphyrin, resulting in bathochromic shifts in the Soret region. Binding constants for the base: porphyrin complexes were determined from steady-state absorption data to be 1743 $\pm$ 68 M^{-1}, 385 $\pm$ 15 M^{-1}, 2433 $\pm$ 150 M^{-1} and 198 $\pm$ 7 M^{-1} for dAMP, dTMP, dGMP and dCMP with T4MPyP respectively. Time resolved fluorescence measurements were used to determine the singlet life-time of T4MPyP in the absence and presence of the nucleotides. The T4MPyP singlet state life-time increased from 5.29 ns to 11.3 ns, 10.3 ns and 7.8 ns in the presence of dAMP, dTMP and dCMP, respectively. In the case of dGMP, the lifetime data could not fit well to two discrete components, rather the data were fit to a distribution centered at 0.69 ns and a discrete component at 3 ns. The quenching is modeled using an excited state reaction mechanism coupled with ground state complexation. This model is consistant with the downward curvature observed for the corresponding Stern-Volmer plot. In the absence of energy transfer, the quenching is attributed to electron transfer between guanine and T4MPyP. A similar trend in fluorescence measurements was observed for the corresponding nucleosides.

Tu-Pos547

Photo-Induced Electron Transfer between Water Soluble Free-Base Porphyrins and Ubiquinone ((R. W. Larsen and S-L. Niu)) Department of Chemistry, University of Hawaii at Manoa, Honolulu HI 96822.

Photo-induced electron transfer (ET) reactions between porphyrins and quinones have received considerable attention due to the critical role of such reactions in photosynthesis and respiration. By far the most widely investigated systems involve covalently linked P-Q molecules designed to probe distance and oreintational dependence of ET. Another usefull yet not so widely investigated system involves diffusional photo-induced ET between P and Q. In this study we report on the presence of a long lived porphyrin π-cation radical subsequent to photo-induced ET between the triplet-state of the anionic free-base 5,10,15,20- tetrakis (4-sulphonatophenyl) porphine (TSPP) and 5,10,15,20- tetrakis (4-carboxyphenyl) porphine (TCPP) and ubiquinone (2,3-dimethoxy-5-methyl-1,4-benzoquinone) (UQ). In contrast, no porphyrin π-cation radical could be detected in the quenching of triplet-state 5,10,15,20-tetrakis(1-methyl-4-pyridyl)porphyrin (TMPyP) by UQ. Examination of the ET reaction in aqueous solution and in a solution containing 5% (w/v) Triton X100 indicates that the reaction occurs between the triplet-state of the porphyrin monomer and UQ with quenching constants of $6x10^9$ $M^{-1}s^{-1}$ and $9.8x10^8$ $M^{-1}s^{-1}$ in aqueous and detergent solutions, respectively. The corresponding quenching rate between the cationic TMPyP and UQ was found to be $3.4x10^9$ $M^{-1}s^{-1}$. A model is presented in which dissociation of the charged separated cage complex is favored in the presence of anionic porphyrins due to charge repulsion of the semi-quinone anion and the negatively charge peripheral groups associated with the anionic porphyrins. In contrast, no dissociation of the cage complex occurs between the cationic porphyrin and semi-quinone due to electrostatic attractions. This results in rapid thermal back electron transfer and no porphyrin π-cation radical is observed.

PHOTOSYNTHETIC REACTION CENTERS

Tu-Pos548

LOW-FREQUENCY RESONANCE RAMAN STUDIES OF HETERO-DIMER MUTANT REACTION CENTERS. ((V. Palaniappan and David F. Bocian)) Department of Chemistry, University of California, Riverside, CA 92521.

Low-frequency resonance Raman (RR) spectra of the primary donor state (D^*) are reported for reaction centers (RCs) from the (M)H202L and (M)H202L/(L)L131H mutants of *Rhodobacter sphaeroides*. Unlike the wild-type RCs, which contain a homodimeric primary donor (P), the primary donor of the mutants is a heterodimer of a bacteriopheophytin (BPh) and a bacteriochlorophyll (BCh). The mutation at (L)L131H position generates a hydrogen-bonding interaction of D_L(BCh) C_9=O group with the histidine. The RR spectra of the mutants were acquired by using a number of excitation wavelengths which span the D^* absorption features. Spectral data were also acquired for the wild-type RCs under similar excitation conditions. At 865-nm-excitation, the (M)H202L RCs exhibit RR features which are characteristic of D_L(BCh) with weak additional contributions from selected D_M(BPh) vibrational modes. In contrast, the double mutant exhibits features due to both D_M(BPh) and D_L(BCh). The RR spectrum of the double mutant also exhibits a significant excitation-wavelength-dependence, unlike either the wild-type or the (M)H202L RCs. In particular, the RR features due to D_M(BPh) observed at 865 nm are significantly attenuated at 850 nm. This suggests that the D* absorption feature of the double mutant consists of two overlapping electronic states.

Tu-Pos549

THE DYNAMICS OF CAROTENOID TRIPLET STATE FORMATION IN *Rhodobacter sphaeroides* REACTION CENTERS. ((Harry A. Frank[1], Veeradej Chynwat[1], Anthony Posteraro[1], Gerhard Hartwich[2], Michaela Meyer[2], Ingrid Katheder[2] and Hugo Scheer[2])) [1]Department of Chemistry, University of Connecticut, Storrs, CT 06269, USA, [2]Botanisches Institut der Universität München, D-80638 München, Germany.

Transient optical studies were carried out at room and low temperatures on several photosynthetic bacterial reaction centers including those from: (a) *Rb. sphaeroides* wild type strain 2.4.1, (b) *Rb. sphaeroides* R-26.1, (c) *Rb. sphaeroides* R26.1 exchanged with pheophytin *a* at the bacteriopheophytin sites and reconstituted with spheroidene, (d) *Rb. sphaeroides* R26.1 exchanged with 13^2-OH-Zn-bacteriochlorophyll at the accessory bacteriochlorophyll sites and reconstituted with spheroidene, and (e) *Rb. sphaeroides* exchanged with [3-vinyl]-13^2-OH-bacteriochlorophyll at the accessory bacteriochlorophyll sites and reconstituted with spheroidene. The rise and decay times of the primary donor and carotenoid triplet-triplet absorption signals were monitored as a function of temperature in the visible wavelength region. For the samples containing carotenoids, all of the decay times correspond well to the previously observed times for spheroidene (~ 3-7 μs). The rise times for the carotenoid triplets in the preparations have been used to determine the activation energies for triplet energy transfer from the primary donor to the carotenoid in the various reaction center preparations. These data will be discussed in terms of the role of the accessory bacteriochlorophyll in triplet state energy transfer from the primary donor to the carotenoid.

Tu-Pos550

KINETICS OF ELECTRON TRANSFER IN ISOLATED REACTION CENTERS DEPENDS ON PROTEIN CONCENTRATION. ((Vladimir P. Shinkarev and Colin A. Wraight)) Department of Plant Biology, University of Illinois, Urbana, IL 61801, USA

The kinetics of light-induced electron transfer in reaction centers (RCs) from the purple photosynthetic bacterium, *Rhodobacter sphaeroides*, were studied in the presence of the detergent lauryldimethylamine-N-oxide. Following the initial light-induced electron transfer from the primary donor (P) to the acceptor quinone complex, the dark re-reduction of P^+ reflects recombination from the reduced acceptor quinones, Q_A and Q_B. We find that the kinetics of the P^+ dark relaxation depend on RC concentration: the lower the RC concentration, the smaller is the time and amplitude of the slow component of the P870 dark relaxation. Because addition of the detergent reverses the effect of decreasing RC concentration we conclude that these changes are due to the interaction of detergent both with RC protein and acceptor quinones. We found that at least three different effects contribute to the observed apparent dependence of the electron transfer on protein concentration: (1) At low detergent concentration RCs form aggregates in which the time of the slow phase of P^+ dark relaxation is faster than in monomers. (2) Also at low detergent concentration, quinone is extracted from the Q_B binding site, resulting in a smaller fraction of the slow phase in comparison with high detergent concentration. (3) At high detergent concentration, extraction of quinone from RC-detergent micelles, in an RC-concentration dependent manner, becomes the dominant effect, leading to a steady decline in the fraction of the slow phase of recovery. These the interactions of the detergent, both with hydrophobic regions of the protein and with quinone, provide the basis for dependence of the kinetics of electron transfer on protein concentration. Supported by NSF.

Tu-Pos551

QUANTITATIVE ANALYSIS OF THE INTERACTION OF DETERGENT WITH REACTION CENTERS OF PURPLE BACTERIA. ((Vladimir P. Shinkarev and Colin A. Wraight)) Department of Plant Biology, University of Illinois, Urbana, IL 61801 USA (Sponsored by E. Takahashi)

A new quantitative approach has been developed to analyze the kinetics of light-induced electron transfer in isolated reaction centers (RCs) from the purple photosynthetic bacterium, *Rhodobacter sphaeroides*, taking into account the exchange of quinone between RC micelles and detergent (lauryldimethylamine-N-oxide) micelles (see accompanying abstract). This analysis has the following key features: (1) Binding of detergent to RCs changes the apparent critical micelle concentration (CMC) for detergent. The apparent CMC for detergent depends on the RC concentration and on the amount of detergent bound to RC; (2) The average number of quinones bound per RC micelle is determined by equilibrium partition between a "RC phase" and a "detergent phase"; (3) The exchange of quinone between different micelles (RC- and detergent micelles) occurs slower than electron transfer from primary quinone acceptor, Q_A^- to photooxidized primary donor, P^+; (4) The exchange of quinone between the detergent "phase" and the Q_B binding site within the same RC micelle is much faster than electron transfer between Q_A^- and P^+. This analysis modifies the interpretation of the kinetics of P^+ dark relaxation, in isolated RCs, in terms of molecular parameters of the system, and accounts for certain discrepancies between experiment and the predictions of previous approaches. In particular, it explains the dependence of the amplitude and time of the slow component of P^+ dark relaxation on the ratio of detergent and RC concentrations (i.e., [detergent]/[RC]) described in accompanying abstract. The effects of detergent and protein concentration described here are expected to be a general phenomenon for detergent-solubilized quinone-dependent electron transfer protein complexes of respiratory and (or) photosynthetic electron transport chains (e.g., cytochrome bc_1 - complexes, quinol oxidases, SDH, NADH-DH, etc.). Supported by NSF.

Tu-Pos552

SURFACE PLASMON RESONANCE STUDIES OF MEMBRANE PROTEINS: TRANSDUCIN BINDING AND ACTIVATION BY RHODOPSIN MONITORED IN THIN MEMBRANE FILMS. ((Z. Salamon, Y. Wang, J.L. Soulages, M.F. Brown and G. Tollin)) Departments of Biochemistry and Chemistry, University of Arizona, Tucson, AZ 85721. (Spon. by M.A. Wells).

In a previous study (Z. Salamon et al., Biochemistry 33, 13706 (1994)), surface plasmon resonance (SPR) spectroscopy was used to monitor rhodopsin incorporation and photobleaching in an egg lecithin membrane supported on a thin silver film. The present experiments utilize SPR to observe binding and activation of transducin (G_t) under these conditions. Prior to rhodopsin photolysis, G_t binds tightly ($K_{eq} \approx 60$ nM) and with positive cooperativity to rhodopsin in the lipid layer to form a closely packed film, with a calculated average thickness of approximately 57Å. G_t binding saturates at a G_t / rhodopsin ratio of approximately 0.6. Upon visible light irradiation, characteristic changes occur in the SPR spectrum, which can be explained by a 6Å increase in the average thickness of the lipid/protein film caused by formation of metarhodopsin II (MII). Upon subsequent addition of GTP, further SPR spectral changes are induced, which are interpreted as resulting from dissociation of the α-subunit of G_t, formation of new MII-G_t complexes, and possible conformation changes in G_t as a consequence of complex formation. The results clearly demonstrate the ability of SPR spectroscopy to monitor and to provide new insights into the biochemical and biophysical events associated with signal transduction in membrane-bound systems.

Tu-Pos553

STRUCTURE OF THE THIRD CYTOPLASMIC LOOP OF BOVINE RHODOPSIN. ((P.L. Yeagle, J.L. Alderfer and A.D. Albert)) Department of Biochemistry, University at Buffalo School of Medicine and Biomedical Sciences, Buffalo, NY 14214 and Department of Biophysics, Roswell Park Cancer Institute, Buffalo, NY 14263

The three-dimensional high resolution structure of rhodopsin is unknown, as is the case for almost all integral membrane proteins. As part of an alternative approach to determination of membrane protein structure, we are pursuing the structure of cytoplasmic domains of this G-protein receptor. A peptide, rhoIII, with the sequence of the third cytoplasmic loop of bovine rhodopsin was synthesized. This soluble peptide was biologically active, inhibiting the light-stimulated activation of the rod cell phosphodiesterase by rhodopsin in rod outer segment disks. RhoIII therefore likely contains structural elements characteristic of native rhodopsin. The solution structure of rhoIII was determined by ^{1}H nuclear magnetic resonance. A defined structure was obtained for about 70% of rhoIII. A model of a turn-helix-turn motif was proposed for the third cytoplasmic loop of rhodopsin, which suggested a molecular switch for activation of the G protein by the receptor.

NEI EY03328

Tu-Pos554

EARLY PHOTOCHEMISTRY SHOWS THE INVOLVEMENT OF ASPARTATE 76 RESIDUE IN SENSORY RHODOPSIN-I FUNCTION. ((I. Szundi and R. A. Bogomolni)) Department of Chemistry and Biochemistry, University of California, Santa Cruz.

Sensory rhodopsin-I (sR-I) free of transducer Htr1 exists in a proton pumping form at higher pH and in a non-pumping one at lower pH (single photon pumping), and its pH dependent behavior has been linked to protonation changes of asp76 residue. The two forms have distinct photocycles. The early steps (K-L-M), are fundamentally different not only from each other but also from the native sR-I, and are sensitive indicators of the protein function. The proton pumping form shows very rapid K-L equilibrium and an M formation within a few microseconds; the non-pumping form has slower K-L equilibrium and significant back conversion to the ground form, and only a partial M formation at very late times (several ms), indicating the lack of a primary proton acceptor in the vicinity of the protonated Schiff's base. Because the photocycle of the asn76 mutant closely resembles that of the non-pumping form we interpret that unprotonated asp76 is the primary proton acceptor in the absence of transducer Htr1. The time-dependent absorption difference spectra were measured in the 100 ns to 1s time window at pH 6.2 and 7.9, and were analyzed using svd, global exponential fit and b-spectra decomposition. Our results show a direct relationship between the photocycle kinetics and protein function, with the primary proton acceptor playing a key role in both the photochemistry and the function of the protein. (Supported by NIH 43561)

Tu-Pos555

ASP76 IS THE SCHIFF BASE PROTON ACCEPTOR IN THE PROTON TRANSLOCATING FORM OF SENSORY RHODOPSIN I ((Parshuram Rath, Elena Spudich[$], John L. Spudich[$] and Kenneth J. Rothschild)) Department of Physics, Boston University, Boston, MA 02215 and [$]Department of Microbiology, University of Texas Medical School, Houston, TX 77030

Sensory rhodopsin I (SRI) exists in a pH dependent equilibrium between two different forms in the absence of its transducer protein HtrI. At pH below 7, it exists primarily in a blue form (λ_{max}=590 nm) which can function as a phototactic signal transducer when complexed with HtrI, while at higher pH it converts to a purple proton transporting form similar to bacteriorhodopsin (BR) (λ_{max}=550 nm). We report ATR-FTIR data obtained from both low and high pH forms of SRI reconstituted into lipid vesicles. The low pH species has an ethylenic C=C stretch mode at 1519 cm^{-1} which shifts to 1527 cm^{-1} in the high pH form. No frequency shift was found for the mutant D76N in agreement with visible absorption measurements. Weak negative/positive bands at 1763/1751 cm^{-1} previously assigned to a perturbation of the C=O stretch mode of Asp76 during S_{373} formation in the low pH form are replaced by a single intense positive band near 1749 cm^{-1} in the high pH form. These results along with the effects of H/D exchange indicate that Asp76 is protonated in the signal transducing form of SRI and is ionized and functions as the Schiff base proton acceptor in the proton transporting form of SRI similar to BR. These results definitively confirm a key aspect of the coupling model for HtrI-control of proton transfer in SRI (J.L. Spudich, (1994), Cell 79, 747-750).

Tu-Pos556

TRYPTOPHAN UV ABSORBANCE CHANGES ACCOMPANYING PHOTOACTIVATION OF RHODOPSIN.

((Steven W. Lin and Thomas P. Sakmar)) Howard Hughes Medical Institute, Rockefeller University, 1230 York Ave., New York, NY 10021.

The UV difference spectrum between rhodopsin and metarhodopsin-II (MII) exhibits characteristic sharp bands at 286, 291, and 295 nm. Previous studies have attributed these bands to tryptophan (Trp) residues. Using site-directed mutagenesis, we have replaced each one of the five Trp residues in bovine rhodopsin by either Tyr or Phe (W265Y/F, W175F, W161F, W126F, and W45F). The mutant rhodopsins were expressed in COS cells, purified, and solubilized in dodecyl maltoside or digitonin. MI/Rho and MII/Rho difference spectra of the Trp mutants were compared with those of wild-type rhodopsin in order to assign the UV spectral difference bands. The assignments of the 286-nm band to Trp-265 and the 291- and 295-nm bands to Trp-126 are suggested based on preliminary data from the mutants. These bands are not observed in the wild-type MI/Rho difference spectrum. Therefore, at least two Trp residues undergo a change in their environments concomitant with MII formation. The implications of the Trp absorbance changes in relation to the conformations of ground-state and photoactivated rhodopsin will be presented.

Tu-Pos557

THE EFFECT OF LONG CHAIN ALCOLHOLS ON THE KINETICS OF THE LATE PHOTOINTERMEDIATES OF RHODOPSIN. ((T.L. Mah, I. Szundi, J.W. Lewis, S. Jäger, and D.S. Kliger)) University of California, Santa Cruz, Santa Cruz, CA 95064.

In a recent paper [Thorgeirsson *et al.* 1993. *Biochemistry* 32:13861-13872.] two possible schemes for the interconversion of late rhodopsin photointermediates were proposed. To distinguish between these two schemes, we have begun experiments in which the late photolysis intermediates are perturbed by various methods. In this work, we describe experiments in which the kinetics of rhodopsin in hypotonically washed ROS disk membranes are perturbed with long chain alcohols. Utilizing singular value decomposition and global exponential fitting, three apparent rates are observed suggesting the presence of four intermediates within the 1 μs to 80 ms time range, in agreement with previous work on unperturbed rhodopsin. By fitting the apparent rates and the corresponding *b*-spectra with realistic spectral shapes for the photointermediates, the microscopic rate constants in the kinetic matrices of the two previously proposed schemes are optimized. The effect of long chain alcohols on the microscopic rate constants are analyzed and discussed in relation to the proposed schemes.

Tu-Pos558

L-*CIS*-DILTIAZEM BLOCKS THE LIGHT-DEPENDENT K CONDUCTANCE OF *PECTEN* HYPERPOLARIZING PHOTORECEPTORS. ((Maria del Pilar Gomez and Enrico Nasi)) Department of Physiology Boston University School of Medicine and Marine Biological Laboratory Woods Hole, MA. (Spon. by M.C. Cornwall)

Hyperpolarizing photoreceptors in the distal retina of the scallop resemble vertebrate rods, not only structurally (the light transducing structure derives from modified cilia), but also functionally: the photocurrent is activated by cGMP and rectifies outwardly because of a voltage-dependent block by divalent cations. Because these light-dependent channels are K-selective and susceptible to block by 4-AP and TEA, they may represent a link between cyclic-nucleotide-gated channels and voltage-gated K channels; a kinship between these two families has been suggested on the basis of aminoacid sequence similarity. To further document the functional similarities between these channels and those of vertebrate photoreceptors, we examined the effects of l-*cis*-diltiazem, the best known antagonist of the light-sensitive conductance in rods. Local extracellular application of l-*cis*-diltiazem produced a swift, rapidly reversible suppression of the photocurrent. The $K_{1/2}$ was ≈450 μM, comparable to that obtained in rods under similar conditions. Intracellular dialysis of lower doses (100 μM) also induced a substantial inhibition. No change in the kinetics or the intensity-response relation of the photocurrent was induced by the drug, indicating that the inhibition results from block of the conductance, rather than impairment of the activating cascade; also, no use-dependence was observed, so that the site of action may not require opening of the channel. The blockage was voltage-dependent, increasing with membrane depolarization regardless of the side of application of the drug. On the assumption that the charged form l-*cis*-diltiazem$^+$ is active, this may suggest that the drug interacts with a site accessible from the intracellular compartment only. Supported by NIH grant RO1 EY-07559.

Tu-Pos559

A SLOW CURRENT INDUCED BY LIGHT IN RHABDOMERIC PHOTORECEPTORS: POSSIBLE RELATION TO I_{CRAC}. ((Maria del Pilar Gomez and Enrico Nasi)) Department of Physiology Boston University School of Medicine and Marine Biological Laboratory Woods Hole MA

In rhabdomeric photoreceptors PLC activation and formation of IP_3 are critical early events in phototransduction, and large Ca transients accompany the light response. In several species, Ca permeation through light-dependent channels is minute, and the increase in cytosolic Ca reflects chiefly internal release; repetitive stimulation in Ca-free media can lead to depletion of Ca stores and exhaustion of the photoresponse. In many cells that utilize the IP_3 signalling pathway, the ability to generate sustained responses and to replenish intracellular stores is mediated by a receptor-operated Ca influx mechanism (I_{crac}). In *Lima* rhabdomeric photoreceptors a slow after-depolarization follows intense light stimulation. Under voltage clamp, a corresponding inward current (I_{slow}) can be reproducibly measured; this current develops with a latency of 5-10 s, reaches a peak amplitude ≈100-200 pA in 30-40 s, and decays in 1-3 minutes. I_{slow} is graded with light intensity, but is wavelength-insensitive, which, together with the sluggish activation, rules out a PDA phenomenon. I_{slow} obtains after replacing Na_o with Li, guanidinium, or NMDG, indicating that it is not due to an electrogenic Na/Ca exchange mechanism. Its reversal potential in normal ionic conditions is ≈+30 mV. I_{slow} can be evoked with extracellular Ca (60 mM) as the sole permeant species; Ba can substitute for Ca but Mg cannot. This slow current resembles I_{crac} described in other cells after IP_3 stimulation, and may play an important role in the homeostasis of the Ca stores implicated in the generation of the photoresponse. Supported by NIH grant EY07559

Tu-Pos560

TYROSINE KINASE ACTIVITY IN RETINAL ROD OUTER SEGMENT MEMBRANES. POSSIBLE RELATION TO PHOSPHOINOSITIDE METABOLISM AND ROD FUNCTIONING. ((I.D. Volotovski, A.M. Sholuh, I.D. Artamonov*, L.A. Baranova)) Institute of Photobiology, Academy of Sciences of Belarus, Minsk 220073, Belarus; *Shemjakin-Ovchinnikov Institute of Bioorganic Chemistry, Russian Academy of Sciences, Moscow 117871, Russia.

Protein tyrosine kinases (PTK) are involved in the regulation of many cellular programs and are responsible for the phosphorylation of various cytoplasmic substrates including phospholipases of γ-family. to propagate a ligand-mediated receptor protein tyrosinase signal via the substrates into the cellular responses. Up to now, no information was obtained on the existence of PTK in vertebrate retinal rods. Using two approaches, it was shown that outer segments of bovine rods (ROS) contain tyrosine kinase activity associated with the disc and plasma membranes. A protein product to be phosphorylated had a molecular mass in the range of 70 kDa. Besides, poly(Glu-Tyr) 4:1, the artificial substrate for tyrosine kinases was markedly phosphorylated when it was added to retinal membrane suspension. The influence of light, ion composition and G-protein on tyrosine kinase activity in ROS was studied. The possible relation of tyrosine kinase-activated phosphorylation with phosphoinositide metabolism in rod outer segment was discussed.

TRANSPORTERS AND CHANNELS: FUNCTIONAL SIMILARITIES

W-AM-SymI-1

STRUCTURE AND FUNCTION OF MOLECULAR WATER CHANNELS. ((A.S. Verkman)) Cardiovascular Research Institute. University of California, San Francisco, CA 94143-0521.

Remarkable progress has been made recently in the identification and characterization of water transporting proteins ("water channels", "aquaporins"). There are at present 5 water channels in mammals, >30 from plants and several from amphibia and bacteria. The water channels are small hydrophobic proteins with sequence homology to MIP; in mammals, the water channels are expressed widely in plasma membranes of epithelial and non-epithelial tissues. The majority of molecular-level information about water transporting mechanisms comes from studies on CHIP28 (AQP1), a 28 kDa glycoprotein that forms tetramers in membranes; recent electron cryo-crystallographic data suggests that each monomer contains 6 helical domains surrounding a central aqueous pathway. Functional analysis shows that CHIP28 monomers function independently as water-selective channels without transporting protons, ions or small solutes. Only mutations in the vasopressin-sensitive water channel (AQP2) have been shown to cause human disease - non-X-linked congenital, nephrogenic diabetes insipidus; the physiological significance of other water channels remains unproven. One mercurial-insensitive water channel has been identified (MIWC, AQP4), which has the unique feature of multiple overlapping transcriptional units. Another homolog transports glycerol > water (GLIP, AQP3). Water channels have been expressed in *Xenopus* oocytes, mammalian and insect cells, and yeast. Major questions in the field are the role of water channels in normal physiology and disease, the existence of water channel regulatory mechanisms, and the determination of structure at atomic resolution.

W-AM-SymI-2

MECHANISM OF MULTIDRUG TRANSPORT.((M. Gottesman)) National Cancer Institute.